Zoological Journal of the Linnean Society, 2023, **XX**, 1–27
https://doi.org/10.1093/zoolinnean/zlad179
Advance access publication 12 December 2023
Original Article

OXFORD

Original Article

A new booid snake from the Eocene (Lutetian) Konservat-Lagerstätte of Geiseltal, Germany, and a new phylogenetic analysis of Booidea

Alessandro Palci[1,2,*], Silvio Onary[3], Michael S.Y. Lee[2,4], Krister T. Smith[5,6], Oliver Wings[7,8], Márton Rabi[8,9] and Georgios L. Georgalis[10]

[1]School of Biological Sciences, University of Adelaide, Adelaide, SA 5000, Australia
[2]South Australian Museum, North Terrace, Adelaide, SA 5000, Australia
[3]Laboratório de Paleontologia, Faculdade de Filosofia Ciências e Letras de Ribeirão Preto, Universidade de São Paulo, Avenida Bandeirantes 3900, 14040-901, Ribeirão Preto, São Paulo, Brazil
[4]College of Science and Engineering, Flinders University, Adelaide, SA 5042, Australia
[5]Department of Messel Research and Mammalogy, Senckenberg Research Institute, Senckenberganlage 25, 60325 Frankfurt am Main, Germany
[6]Faculty of Biological Sciences, Goethe University, Max-von-Laue-Str. 9, 60438 Frankfurt, Germany
[7]Natural History Museum, Fleischstr. 2, 96047 Bamberg, Germany
[8]Natural Sciences Collections, Martin Luther University Halle-Wittenberg, Domplatz 4, 06108 Halle (Saale), Germany
[9]Department of Geosciences, Eberhard Karls Universität Tübingen, Hölderlinstr. 12, Tübingen 72074, Germany
[10]Institute of Systematics and Evolution of Animals, Polish Academy of Sciences, Sławkowska 17, 31-016 Kraków, Poland

ZooBank LSID: urn:lsid:zoobank.org:act:75DD1A6B-57F4-4DFF-9883-E7A684294FFF

[*]Corresponding author. School of Biological Sciences, University of Adelaide, Adelaide, SA 5000, Australia; South Australian Museum, North Terrace, Adelaide, SA 5000, Australia. E-mail: alessandro.palci@adelaide.edu.au

ABSTRACT

We describe two exceptionally preserved fossil snakes from the Eocene Konservat-Lagerstätte of Geiseltal, located in the state of Saxony-Anhalt, Germany. The two snake specimens, GMH LIX-3-1992 and GMH XXXVIII-20-1964, can be confidently identified as booids based on general morphology and were thus compared to other geographically and/or temporally close fossil booids. We found that GMH LIX-3-1992 is morphologically very similar to *Eoconstrictor spinifer*, also from Geiseltal, and to *Eoconstrictor fischeri*, from the middle Eocene of Messel, but differs from both in a number of cranial and vertebral features. Based on these differences we erect the new species ***Eoconstrictor barnesi* sp. nov.**; GMH XXXVIII-20-1964 is very similar to GMH LIX-3-1992 and the two differ only in features that are likely ontogenetic. Phylogenetic analyses of snakes using maximum parsimony and Bayesian inference on datasets inclusive of both morphological and molecular data consistently support a close affinity of *E. barnesi* to *E. fischeri* and *E. spinifer*. Our preferred phylogenetic hypothesis places the three species of *Eoconstrictor* in a clade that is sister to Neotropical Boidae, a result consistent with previous studies. The genus *Eoconstrictor* could provide an important calibration point for molecular clock studies of booids and snakes in general.

Keywords: Eocene; evolution; computed tomography; phylogeny; Serpentes

INTRODUCTION

Articulated, largely complete remains of fossil snakes are extremely rare, and known from only a handful of localities around the world. One of the most famous of these localities is the UNESCO World Heritage Konservat-Lagerstätte of Messel, near Frankfurt am Main, Germany, which has produced some spectacular snake specimens from the early–middle Eocene (late Ypresian–early Lutetian, 47.4–48.3 Mya; Baszio 2004, Schaal and Baszio 2004, Scanferla *et al.* 2016, Smith and Scanferla 2016, 2021, 2022, Smith *et al.* 2018, Scanferla and Smith 2020a, b, Georgalis *et al.* 2021). Another late early or middle Eocene site, located about 300 km north-east of Messel, is that of Geiseltal, in the state of Saxony-Anhalt (Salzmann 1914, Krutzsch 1976, Krumbiegel *et al.* 1983, Franzen 2005), a locality that was

Received 22 November 2022; revised 24 October 2023; accepted 30 October 2023

quarried for brown coal (lignite) between the 17th century and the mid-1990s. These quarrying operations revealed a rich ancient ecosystem, a swampy paratropical forest that may have lasted for about 3.8 Myr based on models of sedimentation and compaction rates of peat in subtropical climates (Georgalis *et al.* 2021). The lignite deposits produced a great quantity of exceptionally well-preserved fossils such as mammals, birds, tortoises, crocodilians, lizards, snakes, amphibians, fishes, insects, and plants (Hummel 1935, Kuhn 1939, 1940, 1944, Haubold 1977, Młynarski 1977, Krumbiegel *et al.* 1983, Roček *et al.* 2014, Hastings and Hellmund 2015, 2017, Georgalis 2017, Mayr 2020, Ring *et al.* 2020, Georgalis *et al.* 2021, Falk *et al.* 2022, Villa *et al.* 2022), that provided key evidence to interpret and understand this ancient Eocene ecosystem. Snake fossils from Geiseltal have been known since the 1920s (Barnes 1927), including articulated skeletons (Kuhn 1939, Georgalis *et al.* 2021). Among this snake assemblage, two species have been named, *Palaeopython ceciliensis* Barnes, 1927, and *Paleryx spinifer* Barnes, 1927. Georgalis *et al.* (2021) recently revised these two species, recognised both as valid, reassigned *Paleryx spinifer* to the genus *Eoconstrictor*, and further identified a third, unnamed form in the Geiseltal assemblage, which they referred to as *Eoconstrictor* cf. *fischeri*.

Here we describe two new exceptionally well-preserved fossil snake specimens from Geiseltal. We provide detailed anatomical descriptions of these two large booids (Booidea *sensu* Pyron *et al.* 2014), compare these specimens to other geographically and temporally close booid snakes, and provide a phylogenetic placement of these in a broadly sampled phylogeny of living and extinct snakes under different optimality criteria (parsimony and Bayesian inference).

Geological setting

The former Geiseltal brown coalfield is located about 20 km south-west of Halle (Saale), in the state of Saxony-Anhalt (Sachsen-Anhalt) in Germany and is today occupied by Lake Geiseltal. This Konservat-Lagerstätte yielded a diverse fossil flora and fauna (e.g. Barnes 1927, Krumbiegel *et al.* 1983). The fossil vertebrate localities (open pit mines) of variable preservational conditions were distributed across three major coal seams deposited in a lush paratropical environment characterized by swamps, peat bogs, and creeks (e.g. Haubold and Thomae 1990). The age of the biota is difficult to constrain beyond late early or middle Eocene (~Lutetian) [Krutzsch 1966, 1970, 1976, Jaeger 1971, Franzen and Haubold 1987, Krutzsch *et al.* 1992; for recent reviews of the stratigraphic age of Geiseltal see Ring *et al.* (2020) and Georgalis *et al.* (2021)].

Due to the acidic geochemical environment produced by the large amount of decaying plant matter, the potential for vertebrate fossil preservation was very limited throughout the sequence, except where there was an influx of carbonate-rich waters coming from nearby springs located in the Muschelkalk limestones uphill and to the south and south-west of the Geiseltal Basin, which acted as a natural buffer (Hellmund 2018). Therefore, the best-preserved material was found in quarries located to the south and south-west.

Systematic palaeontological excavations at several sites were conducted between the late 1920s and 1993. Shortly after, the area of the exhausted coal mines was flooded and is since then underwater (Lake Geiseltal) (Hellmund 2018). In total, the locality of Geiseltal produced over 30,000 remains of fossil vertebrates, and about 125 taxa have been described so far. Remains of invertebrates and plants are also common (Steinheimer and Hastings 2018). Fossil reptiles from the Geiseltal locality include turtles, crocodilians, snakes, and lizards (Hummel 1935, Kuhn 1939, 1940, 1944, Haubold 1977, Młynarski 1977, Krumbiegel *et al.* 1983, Rossmann 2000, Smith 2009, Georgalis 2017, Hastings and Hellmund 2017, Georgalis *et al.* 2021, Villa *et al.* 2022); mammals include marsupials, primates, creodonts, rodents, insectivores, chiropterans, tillodontians, perissodactyls, artiodactyls, and a pholidotan (Krumbiegel *et al.* 1983; Ring *et al.* 2020); several species of extinct birds have also been described (Krumbiegel *et al.* 1983, Steinheimer and Hastings 2018, Mayr 2020), along with amphibians and fish (Krumbiegel *et al.* 1983, Roček *et al.* 2014, Falk *et al.* 2022). Invertebrates are abundant and include mostly gastropods and insects (especially beetles and cockroaches), but some crustaceans (ostracods) have also been recorded (Krumbiegel *et al.* 1983). Plants include horsetails, ferns, cycads, conifers, and abundant angiosperms (37 taxa) (Steinheimer and Hastings, 2018).

Regarding fossil snakes, so far only two species have been named from Geiseltal, *Palaeopython ceciliensis* and *Paleryx spinifer* (currently *Eoconstrictor spinifer*), both described by Barnes (1927). Additional, more complete material from the area was described by Kuhn (1939) and more recently by Georgalis *et al.* (2021). Of the several snake specimens from this locality, many are still in need of a detailed description and taxonomic evaluation.

The two fossil snakes described here come from two fossil sites, identified using Roman numerals as LIX (full site name: 'Mücheln-Südfeld-Fortsetzung'; Hellmund 1997) and XXXVIII (located in the open pit mine Neumark-Süd; Haubold and Thomae 1990). Fossil site XXXVIII yielded the holotype of *E. barnesi*, while fossil site LIX produced the paratype. Both sites were located within the upper middle-coal seam (obere Mittelkohle) (Fig. 1).

Institutional abbreviations

American Museum of Natural History, New York, NY, USA (AMNH); Geiseltalmuseum of Martin-Luther-Universität Halle-Wittenberg, now referred to as the Geiseltalsammlung, housed as part of the Zentralmagazin Naturwissenschaftlicher Sammlungen, Halle, Germany (GMH); Messel vertebrate collection, Senckenberg Research Institute, Frankfurt am Main, Germany (SMF-ME); Yale Peabody Museum, New Haven, CT, USA (YPM); Zoologisches Forschungsmuseum Alexander Koenig, Bonn, Germany (ZFMK).

MATERIAL AND METHODS

Fossil material

The two snake specimens described here are housed in the Geiseltal Collection, formerly known as the Geiseltal Museum (GMH), in the municipality of Halle, Saxony-Anhalt, Germany. The specimens are registered under the acronyms of GMH XXXVIII-20-1964 and GMH LIX-3-1992. The fossils were examined, photographed, and scanned using the high-resolution computed tomography scanner (microCT) Tomoscope

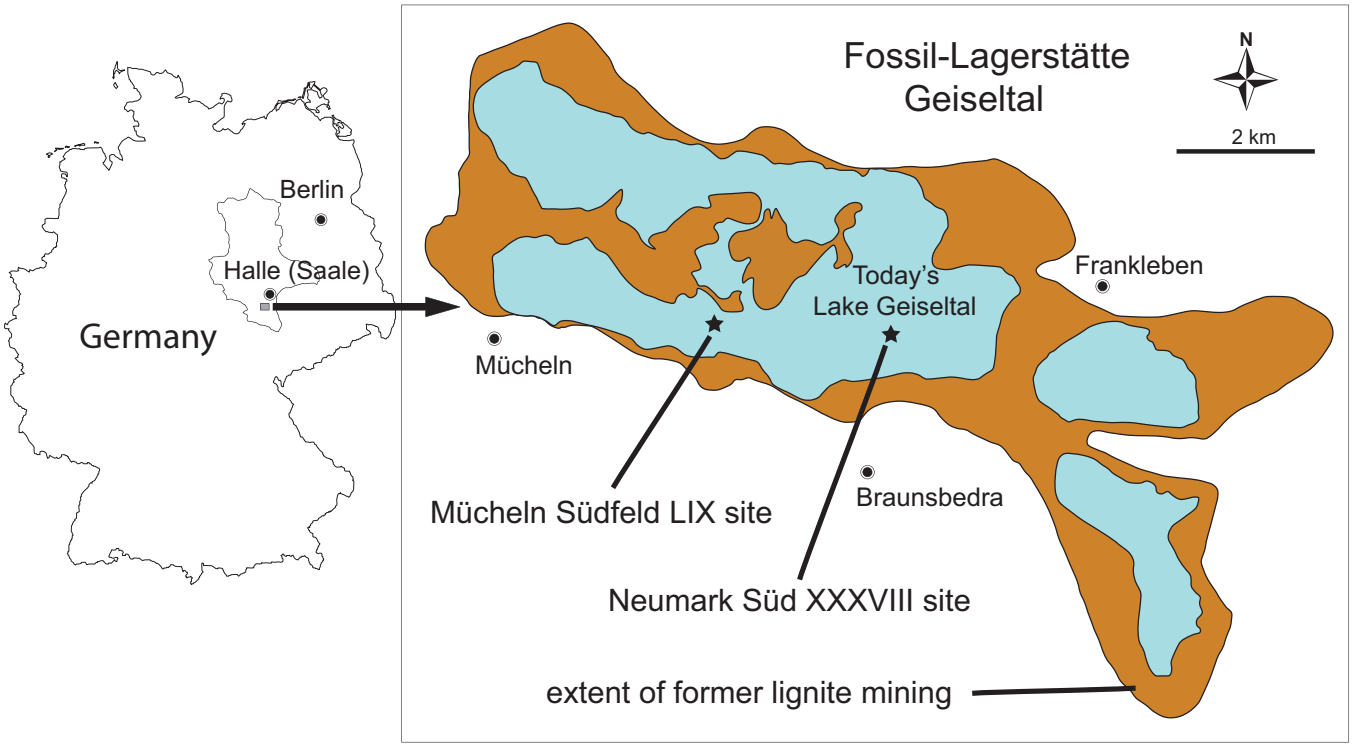

Figure 1. Map of Germany, with close-up on the locality of Geiseltal, in Saxony-Anhalt. The stars mark the two fossil sites that yielded GMH XXXVIII-20-1964 and GMH LIX-3-1992.

HV 500-Werth at the Fraunhofer-Entwicklungszentrum Röntgentechnik (EZRT) of the Fraunhofer-Institut für Integrierte Schaltungen (IIS) in Deggendorf, Bavaria, Germany.

Specimen GMH LIX-3-1992 was scanned at an isometric resolution of 37.5 µm, centered on the skull, whereas GMH XXXVIII-20-1964 was scanned at an isometric resolution of 100.2 µm (the lower resolution was due to limitations imposed by the larger size of the specimen and the field of view of the microCT scanner).

The microCT data were then analysed in Avizo Lite 9.0 (Thermo Scientific™), where all the individual bones that were not too fragmented were digitally isolated via segmentation, to facilitate anatomical description and comparative analyses.

Phylogenetic analyses

In order to test the phylogenetic affinities of the new specimens, GMH LIX-3-1992 and GMH XXXVIII-20-1964 were assessed in a data matrix modified and updated from a recent study by Onary *et al.* (2022) (see Supporting Information, File S1). As in the study by Onary *et al.* (2022) fossil booids were densely sampled, including key taxa such as the European snakes *Messelophis variatus* Baszio, 2004, *Rieppelophis ermannorum* (Schaal & Baszio, 2004), *Eoconstrictor fischeri* (Schaal, 2004), *Eoconstrictor spinifer* (Barnes, 1927), and *Rageryx schmidi* Smith & Scanferla, 2021. The fossil pythonoid *Messelopython freyi* Zaher & Smith, 2020 was also included. The data matrix was edited using Mesquite v.3.0 (Maddison and Maddison 2019).

This new data matrix (Dataset I) consisted of 52 taxa and 240 morphological characters (listed in Supporting Information, File S1). A second dataset (Dataset II) was created combining the morphological data with molecular data from living terminal taxa published in Tonini *et al.* (2016). Both Dataset I and Dataset II were analysed under two distinct optimality criteria, undated Bayesian inference and maximum parsimony (under equal weights), for a total of four main analyses (see main text below, and Supporting Information, File S2). In the primary analyses, all morphological characters were treated as unordered. Thirteen multistate characters formed morphoclines and were alternatively treated as unordered or ordered (see Supporting Information, File S1), to see if ordering resulted in any significant changes to our topologies.

In all the primary analyses above, GMH LIX-3-1992 and GMH XXXVIII-20-1964 were merged into a single terminal taxon, i.e. an operational taxonomic unit (OTU). However, additional analyses were performed where the two specimens were kept as separate OTUs, to test for their individual affinities and identification as a single taxon. In these additional analyses, highly incomplete, phylogenetically unstable (i.e. rogue) taxa, namely *Boavus occidentalis* Marsh, 1871, and *Coniophis precedens* Marsh, 1892, were also included, and analysed using Bayesian and parsimony analyses based on both morphological and molecular data.

Bayesian analyses were conducted using MrBayes v.3.2.7 (Ronquist *et al.* 2012). The analysis of Dataset I (morphology only) was performed employing the Mkv model (Lewis 2001), using gamma rate variation for the morphological partition, whereas for Dataset II (morphology + DNA) the molecular partitions and models were selected using PartitionFinder 2 (Lanfear *et al.* 2017). The analyses using Dataset I were performed applying four independent runs of 50 million generations, where each run used four chains (one heated and three cold) sampled every 5000 generations, with temperature set to

0.1, and the first 20% of the generations discarded as burn-in. For Dataset II the analyses were set with the following parameters: four independent runs of 50 million generations, with six chains (one heated and five cold) per run sampled in every 5000 generations, temperature = 0.1, with Propset commands increasing the time spent on topology moves (see executable file in Supporting Information, File S2), and 50% of the generations discarded as burn-in. Stationarity (convergence) was evaluated using the software Tracer v.1.7 (Rambaut *et al.* 2018) and MrBayes screen outputs: the absolute values of effective sample size for each parameter (ESS > 200), standard deviation of split (clade) frequencies across the runs (SDSF < 0.01), and the potential scale reduction factor (PSRF ~1.0).

Parsimony analyses were performed using PAUP* v.4.0a (Swofford 2003). The most parsimonious trees (MPTs) were retrieved in PAUP* v.4.0a via heuristic search using the following combination of tree-search algorithms: 1000 random addition search replicates, tree-bisection-reconnection (TBR) branch swapping, nchuck = 2000 and chuckscore = 1 (i.e. saving up to 2000 MPTs per replicate). Branch support values were based on 500 bootstrap replicates (each with 50 random addition search replicates, saving up to 1000 trees per replicate).

Character optimization on the preferred topology was performed in PAUP* v.4.0a using parsimony as the optimality criterion. The executable files (with data matrices) for all parsimony and Bayesian analyses are appended as Supporting Information, File S2.

SYSTEMATIC PALAEONTOLOGY

Squamata Oppel, 1811a

Serpentes Linnaeus, 1758

Constrictores Oppel, 1811b (*sensu* Georgalis and Smith 2020)

Booidea Gray, 1825 (*sensu* Pyron *et al.* 2014)

Genus *Eoconstrictor* Scanferla & Smith, 2020a

Type species: Palaeopython fischeri Schaal, 2004 (original combination), currently *Eoconstrictor fischeri* (Schaal, 2004) following the work of Scanferla and Smith (2020a).

Type species locality and age: Messel Pit, Germany (Smith *et al.* 2018). All known specimens of *E. fischeri* come from the lacustrine 'oil-shale' of the Middle Messel Formation (near the Ypresian–Lutetian boundary, ~48 Mya) (Lenz *et al.* 2015).

Emended diagnosis: Eoconstrictor can be distinguished from all other snakes in having the following combination of features: edentulous premaxilla with bifid vomerine processes (unique autapomorphy); prootic with dorsoventrally compressed opening for exit of maxillary branch of trigeminal nerve (V2), posterior margin of this foramen pointed (unique autapomorphy); between one and four labial foramina on the maxilla; 15–18 maxillary teeth; palatine with 5–6 teeth; pterygoid with 10–11 teeth; dentary with 17–19 teeth; midsagittal keel along the ventral side of the basioccipital contributing to V-shaped cross-section (adult feature, may be absent in juveniles); ectopterygoid process of pterygoid merging anteriorly with dentigerous process via gently concave (almost straight) margin (i.e. no deep emargination between dentigerous ramus and ectopterygoid process). This feature, in combination with a broad basipterygoid flange located immediately opposite on the medial side, gives the mid-portion of the pterygoid a broad, diamond-shaped to sub-elliptical appearance in dorsoventral view; total vertebral count up to 369 vertebrae, of which *c.* 246–303 are precloacal vertebrae, three are cloacal vertebrae (three vertebrae with lymphapophyses are visible in *E. fischeri* SMF-ME 1607), and up to *c.* 71 are caudal vertebrae. *Eoconstrictor* can be differentiated from *Palaeopython* Rochebrune, 1880, in having a thinner zygosphene bearing a prominent median lamellar tubercle, and in lacking a palatine foramen and a sigmoidal lateral margin of the maxilla (in dorsal view). *Eoconstrictor* can be differentiated from *Paleryx* Owen, 1850, in lacking a palatine foramen, in having a comparatively taller neural spine (especially on posterior trunk vertebrae), and in lacking a depressed neural arch on posterior trunk vertebrae. *Eoconstrictor* further differs from *Phosphoroboa* Georgalis, Rabi & Smith, 2021, in having a lower pterygoid tooth count (10–11 vs. 14), in lacking an anteromedial projection of the pterygoid at the palatine articulation, and in having a generally U-shaped frontoparietal suture (rather than V-shaped).

Remarks: The number of precloacal vertebrae is best known in the type species of the genus, *E. fischeri* (cf. Schaal 2004 and Smith and Scanferla 2022). SMF-ME 1004 and SMF-ME 2504 have a very high number of vertebrae (around 300 precloacals in SMF-ME 2504), whereas SMF-ME 1607 has notably fewer (around 246 precloacals). Given the stratigraphic distribution of these specimens, the variation does not seem to indicate secular change through time. SMF-ME 1002 is from 1–3 m above marked bed Alpha, SMF-ME 2504 is from 6–3 m below Alpha (at *c.* 7000 yr/m, 28,000–63,000 years apart), and SMF-ME 1607 is from in between.

Based on data from Szyndlar and Georgalis (2023) on the minimum and maximum number of precloacal vertebrae in non-Caenophidian snakes (Supporting Information, File S3), precloacal variability [calculated as (Max—Min)/Min, where Max = maximum number of precloacals and Min = minimum number of precloacals] ranges between 0 and 0.5. *Eoconstrictor fischeri*, with a variability of (303 – 246)/246 = 0.23, would thus be close to the median value (Supporting Information, File S1: Fig. S3).

Eoconstrictor barnesi sp. nov.

(Figs 2–10, Supporting Information, File S1: Figs S1, S2)

Zoobank registration: This published work and the nomenclatural act it contains have been registered in ZooBank, the official registry of zoological nomenclature for the International Code of Zoological Nomenclature (ICZN). The ZooBank LSIDs (Life Science Identifiers) can be resolved and the associated information viewed through any standard web browser by appending the LSID to the prefix 'https://zoobank.org/'. The LSID for this publication is: urn:lsid:zoobank.org:pub:7EA0164B-217B-49AD-88FC-20F231060251, while the LSID

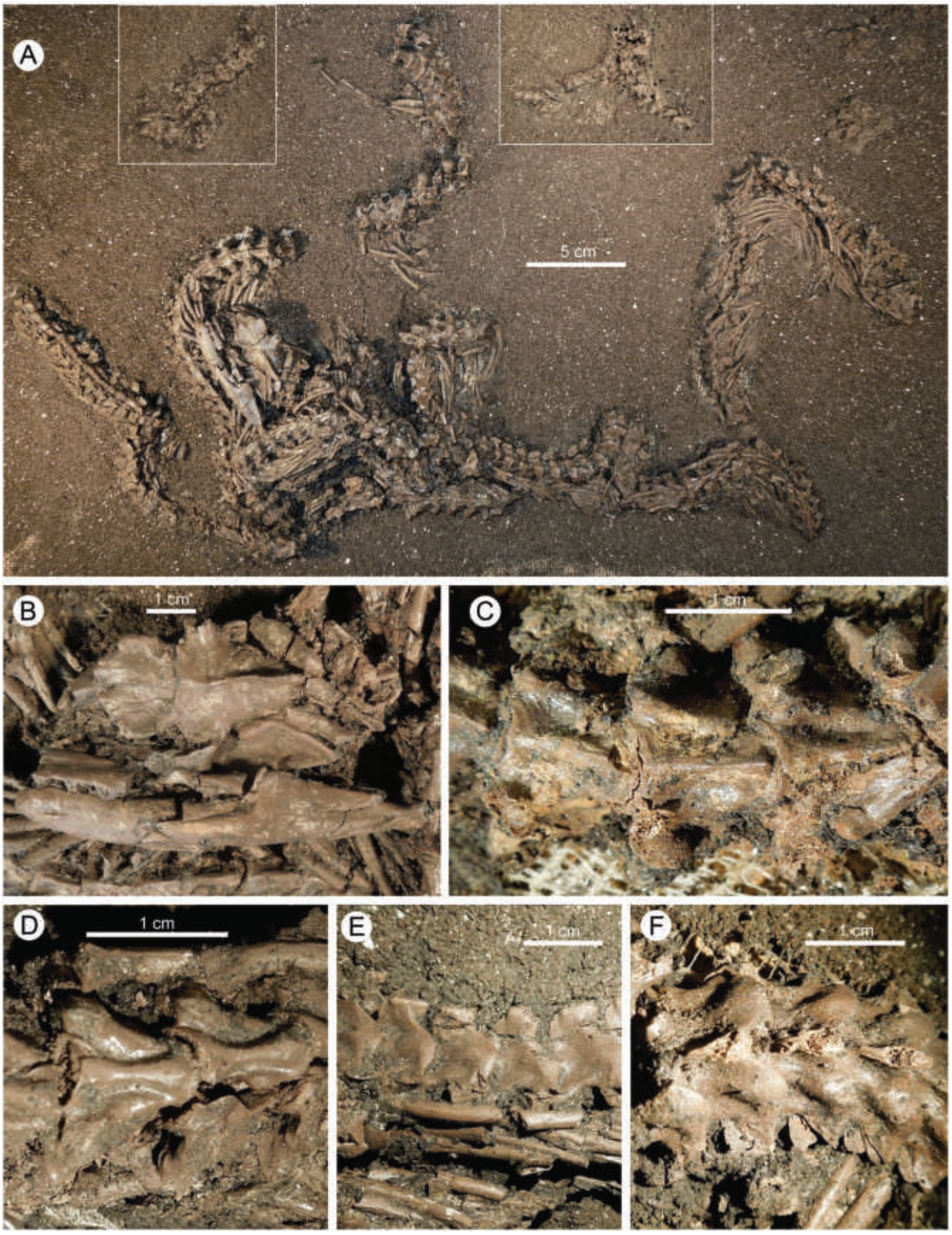

Figure 2. *Eoconstrictor barnesi*, GMH XXXVIII-20-1964, holotype. A, View of the specimen as preserved, insets show clusters of vertebrae that are preserved on the same slab but a few centimetres away from the rest of the body; (B) close-up of the skull in dorsal view and disarticulated left lower jaw in lateral view; (C) close-up of three mid-trunk vertebrae in ventral view; (D) close-up of two posterior trunk vertebrae in ventral view; (E) close-up of four mid-trunk vertebrae in left lateral view; (F) close-up of four mid-trunk vertebrae in dorsal view.

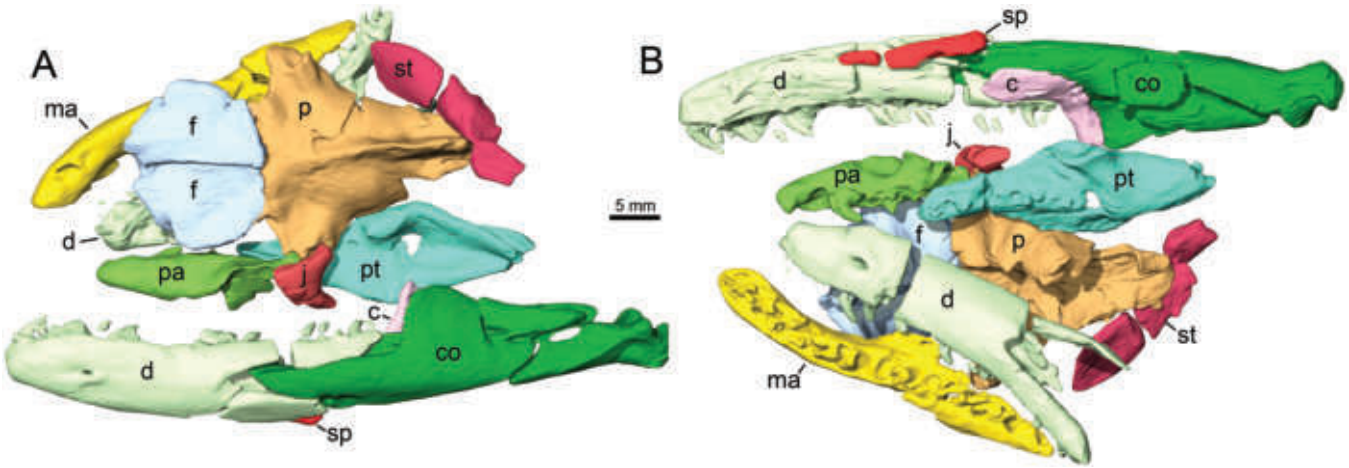

Figure 3. *Eoconstrictor barnesi*, GMH XXXVIII-20-1964, holotype, digital renderings of the segmented skull. A, skull in dorsal view and disarticulated left lower jaw in lateral view. B, skull in ventral view and disarticulated left lower jaw in medial view. Abbreviations: c, coronoid; co, compound; d, dentary; f, frontal; j, fragment of jugal?; ma, maxilla; p, parietal; pa, palatine; pt, pterygoid; sp, splenial; st, supratemporal.

for the new species *Eoconstrictor barnesi* is: urn:lsid:zoobank.org:act:75DD1A6B-57F4-4DFF-9883-E7A684294FFF

Etymology: Species epithet honouring Ben Barnes, who pioneered palaeontological excavations and research in the brown coal deposits of Geiseltal in the 1920s, as part of his Ph.D. studies at the Geological Institute of Halle (Saale).

Holotype: GMH XXXVIII-20-1964, a partial skull and partially disarticulated skeleton missing only the most anterior precloacal region, the cloacal region, and most of the tail (Figs 2–5, Supporting Information, File S1: Fig. S1).

Paratype: GMH LIX-3-1992, a moderately complete and only slightly disarticulated skull and skeleton preserving the anterior half of the body (Figs 6–10, Supporting Information, File S1: Fig. S2).

Type locality and age: The Konservat-Lagerstätte of Geiseltal, located about 30 km west of Leipzig and 20 km south-east of Halle, in the state of Saxony-Anhalt, Germany (Barnes 1927, Krumbiegel *et al.* 1983). The fossils were recovered from fossil sites within coal mines identified by Roman numerals (e.g. LIX, XXXVIII). Both fossil specimens come from fossil sites in the upper middle coal seam (obere Mittelkohle). The age of the deposits is broadly estimated as late early or middle Eocene (~Lutetian, i.e. anywhere between 41 and 48 Mya) (Georgalis *et al.* 2021).

Diagnosis: Eoconstrictor barnesi sp. nov. can be distinguished from *E. fischeri* based on the presence of a single labial foramen in the maxilla (four in *E. fischeri*), the different position of the mental foramen, which is located ventral to the 4th tooth position (ventral to the 5th tooth position in *E. fischeri*), and based on the lateral offset of the mandibular cotyle relative to the rest of the compound bone (offset absent in *E. fischeri*). *Eoconstrictor barnesi* shares the presence of a single labial foramen in the maxilla with *E. spinifer*, but can be distinguished from the latter based on: its more elongated maxilla (length/height ratio between 7.5 and 7.9 vs. a ratio of ~4.68 in *E. spinifer*; the maxilla of *E. spinifer* is slightly damaged posteriorly, but based on its posterior tapering no more than two tooth positions are missing); a quadrate ramus of the pterygoid that is gently curved laterally (forming a distinct ~120° angle in *E. spinifer*); the presence of a median tubercle on the zygosphene (absent in *E. spinifer*, at least in the anterior precloacal vertebrae, more posterior vertebrae are unknown in that species); an almost straight anterior margin of the zygosphene (excluding lateral projections) [crenate *sensu* Auffenberg (1963) in *E. spinifer*]; and presence of prezygapophyseal accessory processes throughout the precloacal vertebral column (absent at least in the anterior precloacal vertebrae in *E. spinifer*). *Eoconstrictor barnesi* differs from both *E. fischeri* and *E. spinifer* in the presence of small paracotylar foramina on at least some of its vertebrae and in the anterior margin of the foramen for the exit of the mandibular branch of the trigeminal (V3), which is gently rounded instead of sharply pointed. Although *E. fischeri* and *E. spinifer* share a ventromedian crest on the basioccipital (Scanferla and Smith 2020a, Georgalis *et al.* 2021), this element is currently unknown in *E. barnesi*.

Description

Cranial material of GMH XXXVIII-20-1964 (holotype)

Based on the relative length of the lower jaw, the skull of this specimen is about 35% larger than that of the paratype (GMH LIX-3-1992) but unfortunately far less complete (Figs 2B, 3). The only bones that are present and not too badly crushed are the frontals, parietal, left jugal, right supratemporal, right maxilla, left palatine and pterygoid, most of the left lower jaw (missing only the angular), and the right dentary.

The frontals are fairly well preserved, except ventrally, where the descending flanges and medial pillars are broken off (Fig. 4A–D). However, a portion of the medial frontal pillars is still preserved dorsally, indicating that these were present. In dorsal view each frontal has an almost semicircular outline, with a distinct lateral flange above the orbit. In lateral view, the frontals show distinct articular surfaces for the prefrontals and the parietal, and the descending flanges, although partially damaged, were clearly deeper posteriorly.

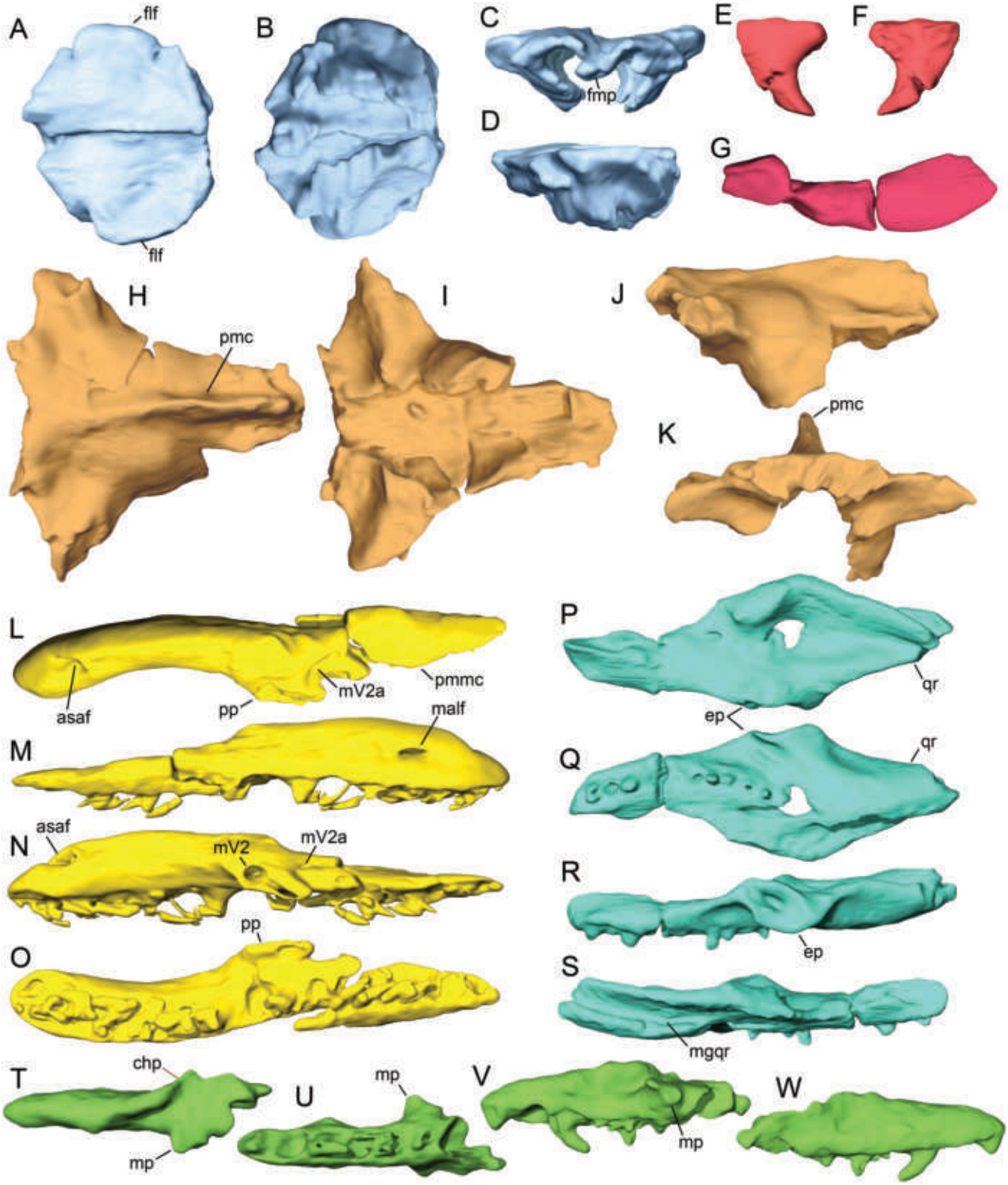

Figure 4. *Eoconstrictor barnesi*, GMH XXXVIII-20-1964, holotype, digital renderings of the segmented skull bones. A–D, frontals in dorsal (A), ventral (B), anterior (C), and left lateral (D) view; E–F, possible fragment of left jugal in lateral (E) and medial (F) view; G, right supratemporal in lateral view; H–K, parietal in dorsal (H), ventral (I), left lateral (J), and anterior (K) view; L–O, right maxilla in dorsal (L), lateral (M), medial (N), and ventral (O) view; P–S, left pterygoid in dorsal (P), ventral (Q), lateral (R), and medial (S) view; T–W, left palatine in dorsal (T), ventral (U), lateral (V), and medial (W) view. Abbreviations: asaf, anterior superior alveolar foramen; bv, blood vessel; chp, choanal process; ep, ectopterygoid process of pterygoid; flf, frontal lateral flange; fmp, frontals median pillars; malf, maxillary labial foramen; mp, maxillary process; mgqr, medial groove on quadrate ramus; mV2, maxillary foramen for maxillary branch of trigeminal nerve (V2); mV2a, accessory foramen for maxillary branch of trigeminal nerve (V2); pmc, parietal midsagittal crest; pmmc, posteromedial maxillary crest; pp, palatine process of maxilla; mV2, maxillary foramen for maxillary branch of trigeminal nerve (V2); qr, quadrate ramus of pterygoid.

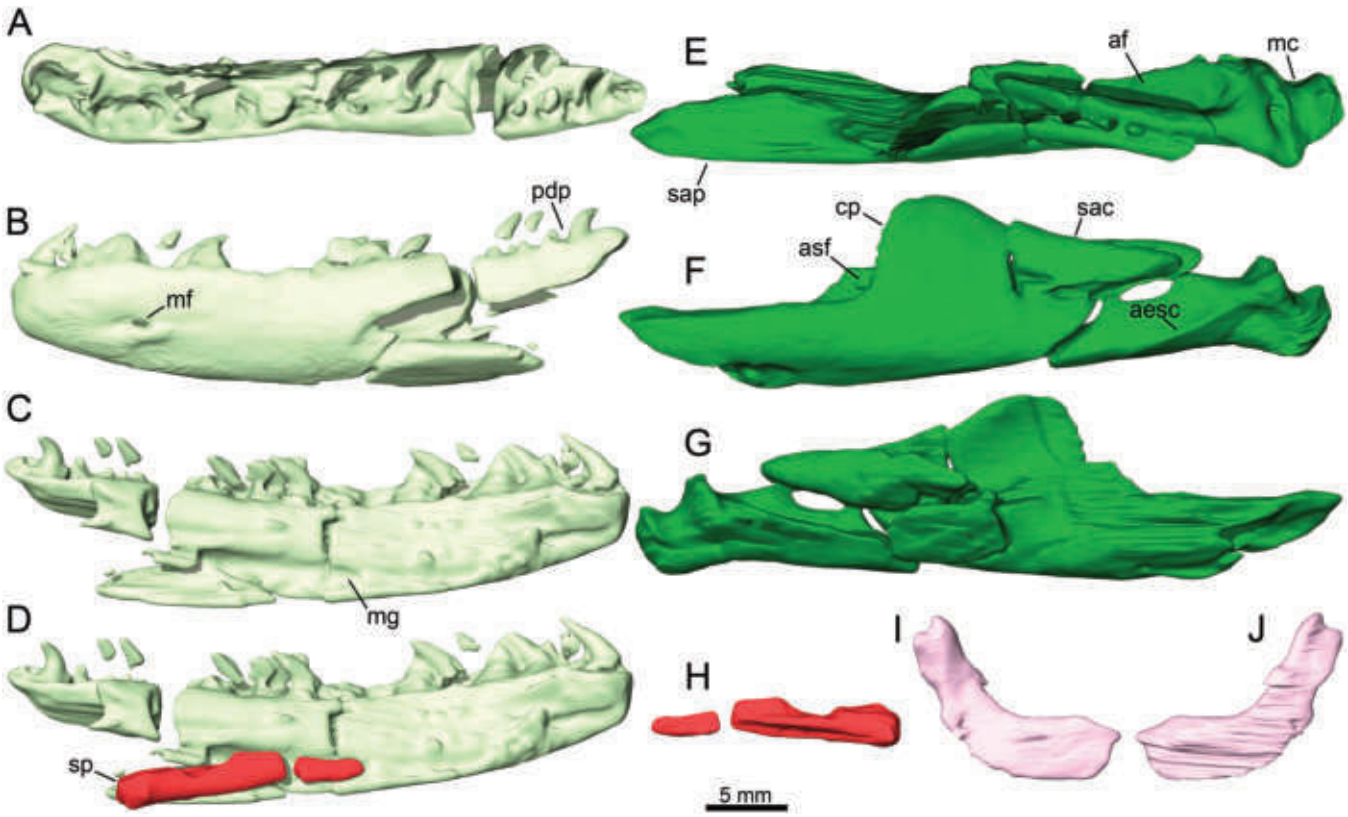

Figure 5. *Eoconstrictor barnesi*, GMH XXXVIII-20-1964, holotype, digital renderings of the segmented lower jaw bones. A–C, left dentary in dorsal (A), lateral (B), and medial (C) view; (D) left dentary in medial view with associated splenial in articulation; (E–G) left compound bone in dorsal (E), lateral (F), and medial (G) view; (H) splenial in medial view; (I–J) left coronoid in medial (I) and lateral (J) view. Abbreviations: aesc, crest for attachment of adductor externus superficialis muscle on compound bone; af, adductor fossa; asf, anterior surangular foramen; cp, coronoid process; pdp, posterodorsal dentary process; mc, mandibular condyle; mf, mental foramen; mg, Meckelian groove; sac, surangular crest; sap, surangular process; sp, splenial.

Unlike the paratype, this specimen also preserves the ventral portion of the left jugal (*sensu* Palci and Caldwell 2013). The dorsal part that articulated between the frontal and the parietal is missing (Figs 3, 4E–F). The preserved part of the element has a claw-shaped profile, with a broad dorsal end (incomplete) and a tapering descending ramus that is recurved posteriorly. The element closely resembles the ventral half of the jugal in *E. fischeri* SMF-ME 11 398.

The right supratemporal is very similar to that of the paratype, has the same dorsomedial curvature, expanded and gently rounded anterior end, and thick posterior end bearing a broad facet for articulation with the quadrate (Fig. 4G).

The parietal is nearly complete and very robust (Fig. 4H–K). Compared to the parietal of the paratype it is relatively broader anteriorly, and more triangular in dorsal view. A distinct mid-sagittal crest is present on the posterior half of this bone and is replaced anteriorly by a round crest that merges into a subtriangular mound just posterior to the frontoparietal suture. The frontoparietal suture appears straighter in the holotype compared to the paratype, where it is clearly U-shaped (i.e. distinctly concave anteriorly). This difference is unlikely to be an artefact of poor preservation of the anterior margin of the parietal, since the only gently curved posterior margin of the frontals matches the anterior margin of the parietal, indicating that this is the genuine morphology present in the holotype.

The right maxilla is quite robust but still relatively elongate (length to height ratio = 7.5). Its ventral margin is straight and bears 17 tooth positions, whereas the dorsal margin has a distinctive sigmoidal curvature in lateral view (Fig. 4L–O), which is absent in the paratype GMH LIX-3-1992 (note that this sigmoidal curvature is not the same as that observed in Messelopythonidae, where the curvature affects the lateral margin of the maxilla and is observed in dorsal view; Smith and Scanferla 2022). However, as in the paratype, the maxilla of GMH XXXVIII-20-1964 also bears an anterior superior alveolar foramen that is located dorsal to the third maxillary tooth position, and has two foramina for the entry of the maxillary division of the trigeminal nerve (V2). The main, larger entrance of the trigeminal nerve in the maxilla is located on the medial end of the palatine process, whereas a foramen for a secondary smaller branch is located just posterior to this process, near its base. The palatine process is quadrangular in shape and anteromedially long. As in the paratype, the maxilla of GMH XXXVIII-20-1964 also has a thin medial crest running along the posteromedial margin, where this bone would articulate with the ectopterygoid. In dorsal view the maxilla is relatively straight posteriorly, and gently curved medially in the anterior region.

The left pterygoid is relatively well preserved and only lacks the distal half of the quadrate ramus and a small fragment just posterior to the dentigerous portion (Fig. 4P–S). The dentigerous

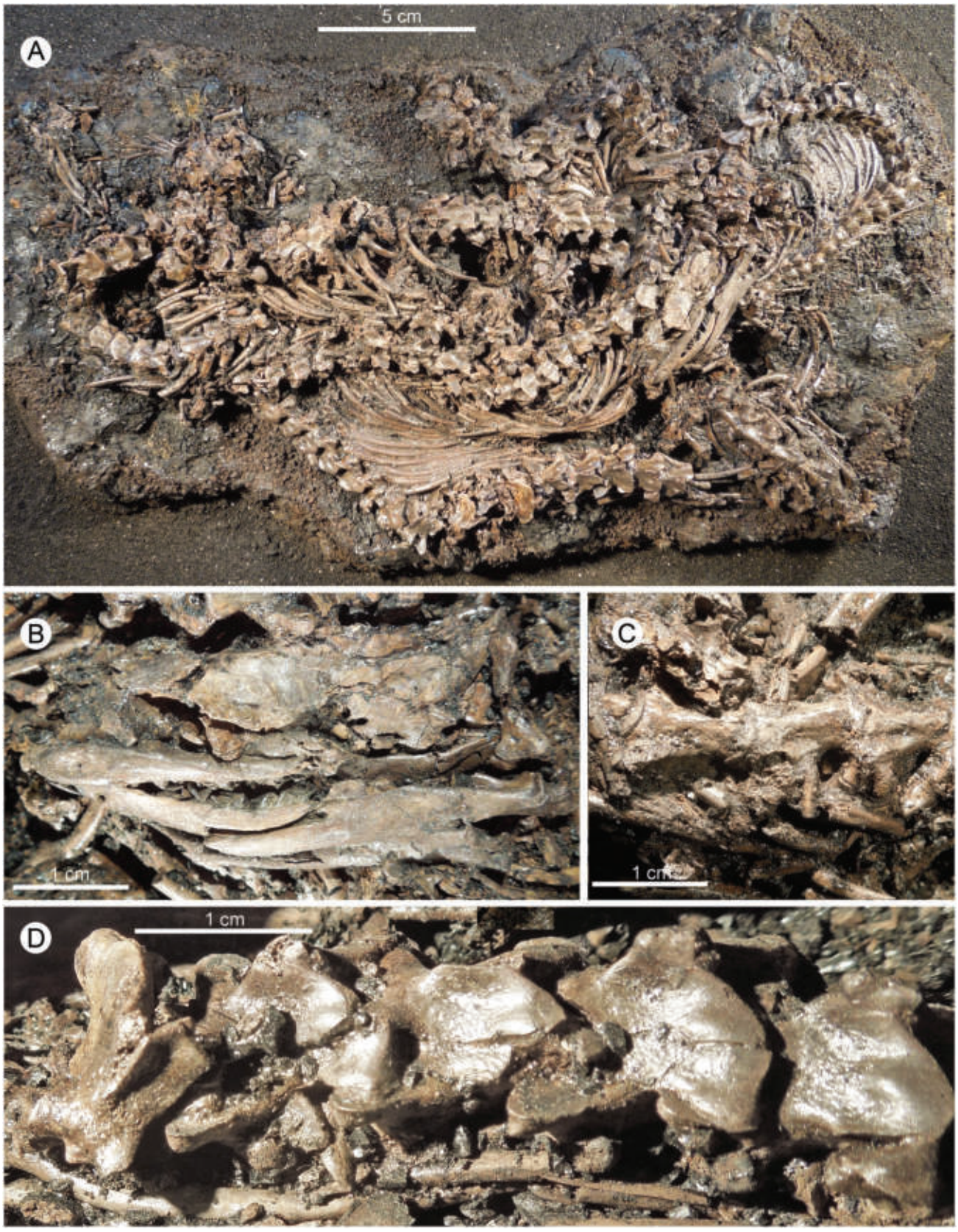

Figure 6. *Eoconstrictor barnesi*, GMH LIX-3-1992, paratype. A, View of the specimen as preserved; (B) close-up of the skull in left lateral view; (C) close-up of three precloacal vertebrae in ventral view; (D) close-up of five precloacal vertebrae in left dorsolateral and dorsal views.

ramus preserves 10 tooth positions and has a concave medial margin. An additional tooth may have been present at the end of the dentigerous ramus, where the bone is damaged. The pterygoid is broadest at the level of the ectopterygoid process, which is quite robust and terminates in a broad sub-elliptical facet for articulation with the ectopterygoid. The longitudinal axis of this facet is

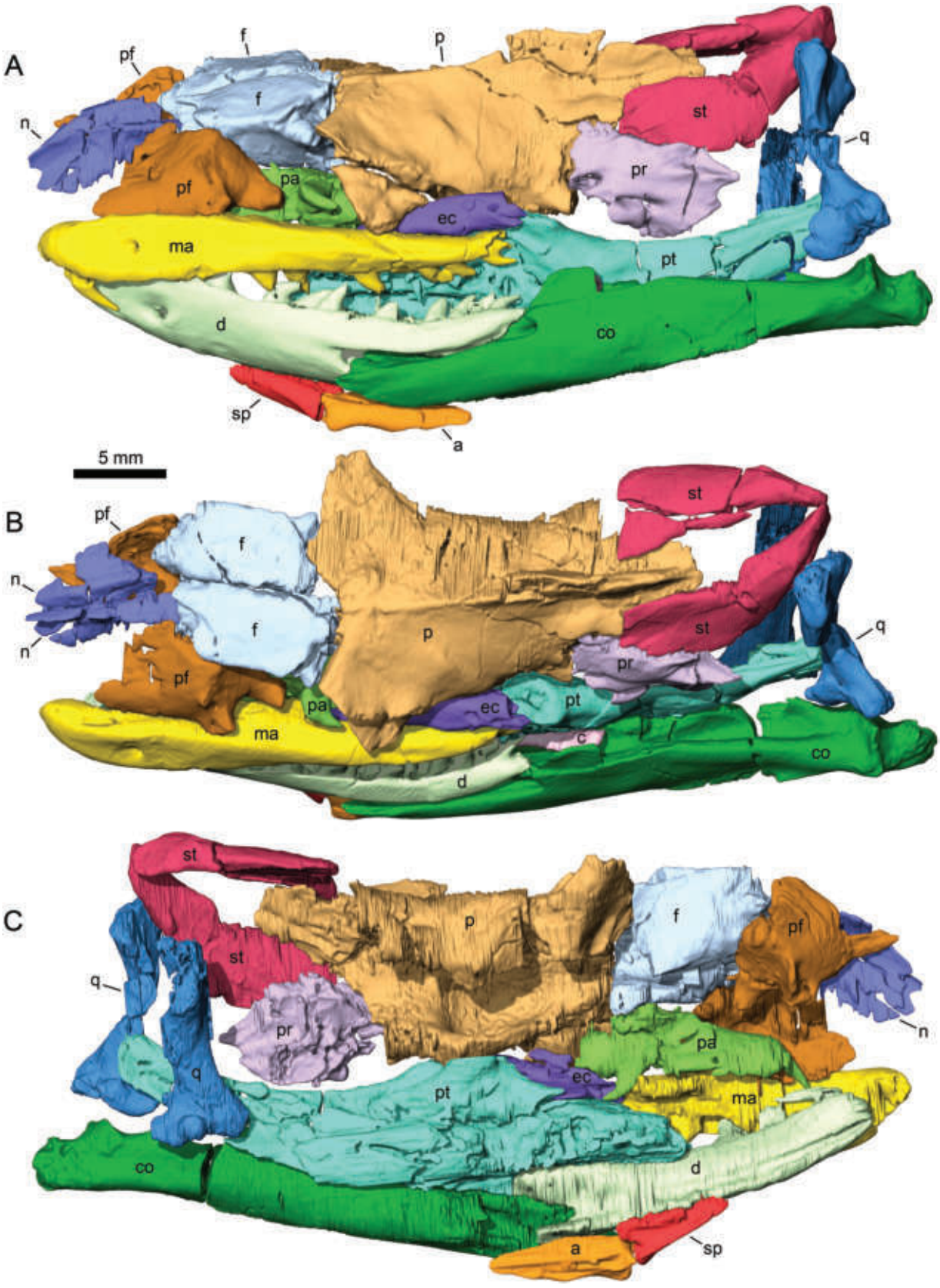

Figure 7. *Eoconstrictor barnesi*, GMH LIX-3-1992, paratype, digital renderings of the segmented skull. A, skull in left lateral view; (B) skull in dorsal view; (C) skull in right ventrolateral view. Abbreviations: a, angular; c, coronoid; co, compound; d, dentary; ec, ectopterygoid; f, frontal; ma, maxilla; n, nasal; p, parietal; pa, palatine; pf, prefrontal; pr, prootic; pt, pterygoid; q, quadrate; sp, splenial; st, supratemporal.

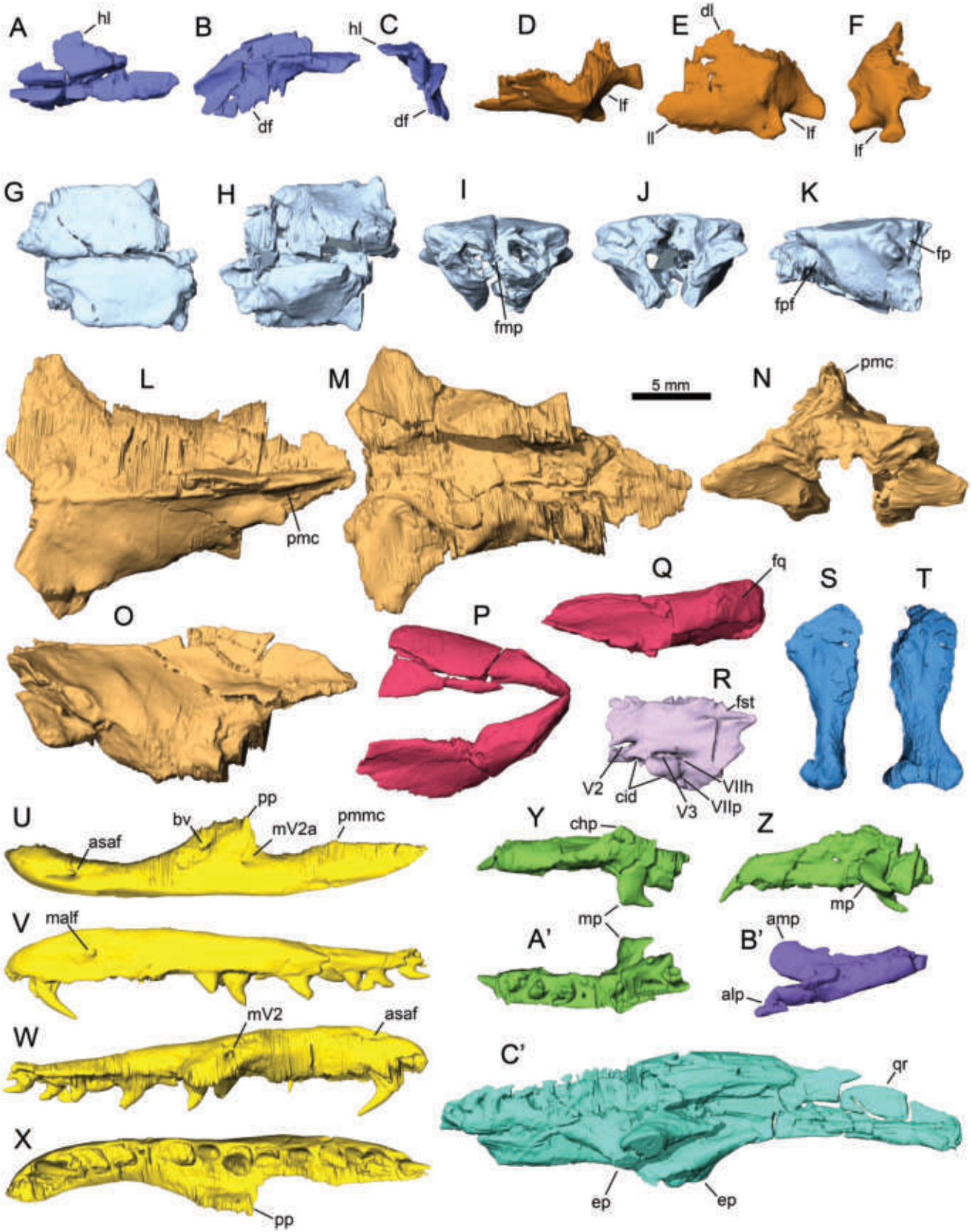

Figure 8. *Eoconstrictor barnesi*, GMH LIX-3-1992, paratype, digital renderings of the segmented skull bones. A–C, nasals in dorsal (A), lateral (B), and anterior (C) view; (D–F) left prefrontal in dorsal (D), lateral (E), and posterior (F) view; (G–K) frontals in dorsal (G), ventral (H), anterior (I), posterior (J), and left lateral (K) view; (L–O) parietal in dorsal (L), ventral (M), anterior (N), and left lateral (O) view; (P–Q) supratemporals in dorsal (P) and left lateral (Q) view; (R) prootic in left lateral view; (S–T) right quadrate in lateral (S) and posterior (T) view; (U–X) left maxilla in dorsal (U), lateral (V), medial (W), and ventral (X) view; (Y–Z, A') left palatine in dorsal (Y), lateral (Z), and

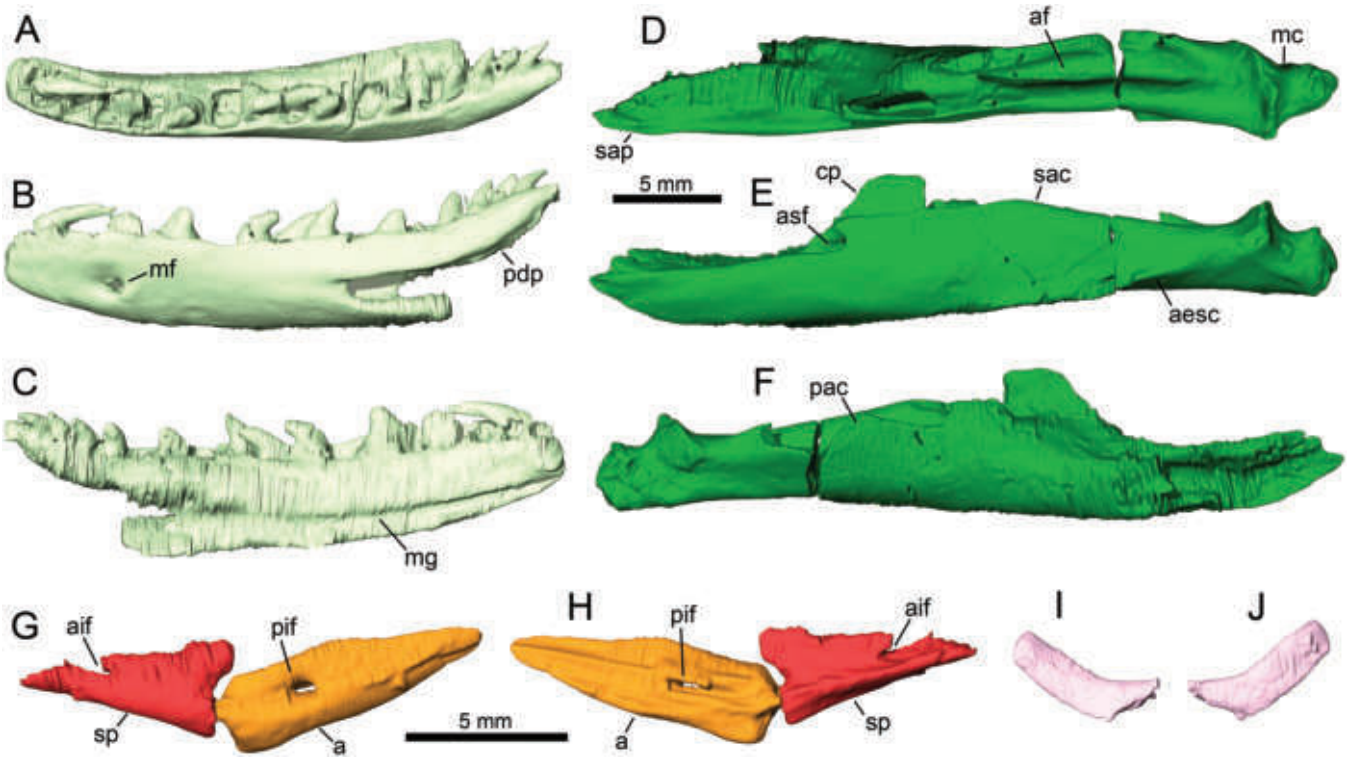

Figure 9. *Eoconstrictor barnesi*, GMH LIX-3-1992, paratype, digital renderings of the segmented lower jaw bones. A–C, left dentary in dorsal (A), lateral (B), and medial (C) view; (D–F) left compound bone in dorsal (D), lateral (E), and medial (F) view; (G) right splenial and angular in medial view; (H) right splenial and angular in lateral view (i.e. showing sutural contacts with dentary and compound, respectively); (I–J) left coronoid in medial (I) and lateral (J) view. Abbreviations: a, angular; aesc, crest for attachment of adductor externus superficialis muscle on compound bone; af, adductor fossa; aif, anterior intermandibularis nerve foramen; asf, anterior surangular foramen; cp, coronoid process; mc, mandibular condyle; mf, mental foramen; mg, Meckelian groove; pac, prearticular crest; pdp, posterodorsal process of dentary; pif, posterior intermandibularis nerve foramen; sac, surangular crest; sap, surangular process; sp, splenial.

tilted anterodorsally. On the opposite side of the ectopterygoid process, the pterygoid expands into a broad rounded flange (basipterygoid flange). The quadrate ramus is relatively deep, at least anteriorly where it is preserved, and bears a deep medial longitudinal groove for the m. protractor pterygoidei.

The left palatine bears six tooth positions and a distinct maxillary process posterolaterally (Fig. 4T–W). This process is short and square in shape, and slightly damaged distally. The choanal process lies on the opposite side, and appears to be very short. There is the possibility that the process may be broken off distally, but its similarity to the same process in the paratype suggests that this may in fact be the actual morphology of the bone. A distinct ridge runs dorsally along the anteromedial edge of the choanal process and merges anteriorly with the dorsal surface of the dentigerous process of the palatine. A distinct concave facet for a tongue-in-groove articulation with the pterygoid is visible at the posterior end of the palatine in ventral view. In medial and lateral views, the palatine is deeper at mid-length and its dorsal margin slopes gently anteriorly and posteriorly. There is no foramen for the passage of a branch of the trigeminal nerve. This palatine is overall very similar to an isolated palatine (YPM-VPPU 12281) from the Phosphorites du Quercy, France, figured in Georgalis *et al.* (2021: fig. 105).

Lower jaw of GMH XXXVIII-20-1964 (holotype)

The lower jaw of this specimen is reasonably complete, missing only the angular (Fig. 5). The left dentary is the better preserved

ventral (A') view; (B') ectopterygoid in dorsal view; (C') overlapping pterygoids, right pterygoid in ventrolateral view obscuring most of left pterygoid lying underneath (in dorsolateral view). Abbreviations: alp, anterolateral process of ectopterygoid; amp, anteromedial process of ectopterygoid; asaf, anterior superior alveolar foramen of maxilla; bv, foramen for blood vessel; chp, choanal process of palatine; cid, foramina for exit (posterior) and re-entry (anterior) of nerve that innervates the constrictor internus dorsalis musculature; df, descending flange of nasal; dl, dorsal lappet of prefrontal; ep, ectopterygoid process of pterygoid; fmp, frontals median pillars; fpf, facet for articulation with prefrontal; fp, facet for articulation with parietal; fq, facet for articulation with quadrate; fst, facet for articulation with supratemporal; hl, horizontal lamina of nasal; lf, lacrimal foramen; ll, lateral lamina of prefrontal; malf, maxillary labial foramen; mp, maxillary process of palatine; mV2a, maxillary foramen for accessory branch of maxillary division of trigeminal nerve (V2); mV2, maxillary foramen for maxillary division of trigeminal nerve (V2); pmc, parietal midsagittal crest; pmmc, posteromedial maxillary crest; pp, palatine process of maxilla; qr, quadrate ramus of pterygoid; V2, exit for maxillary branch of trigeminal nerve (cranial nerve V); V3, exit for mandibular branch of trigeminal nerve; VIIh, exit for hyomandibular branch of facial nerve (cranial nerve VII); VIIp, exit for palatine branch of facial nerve.

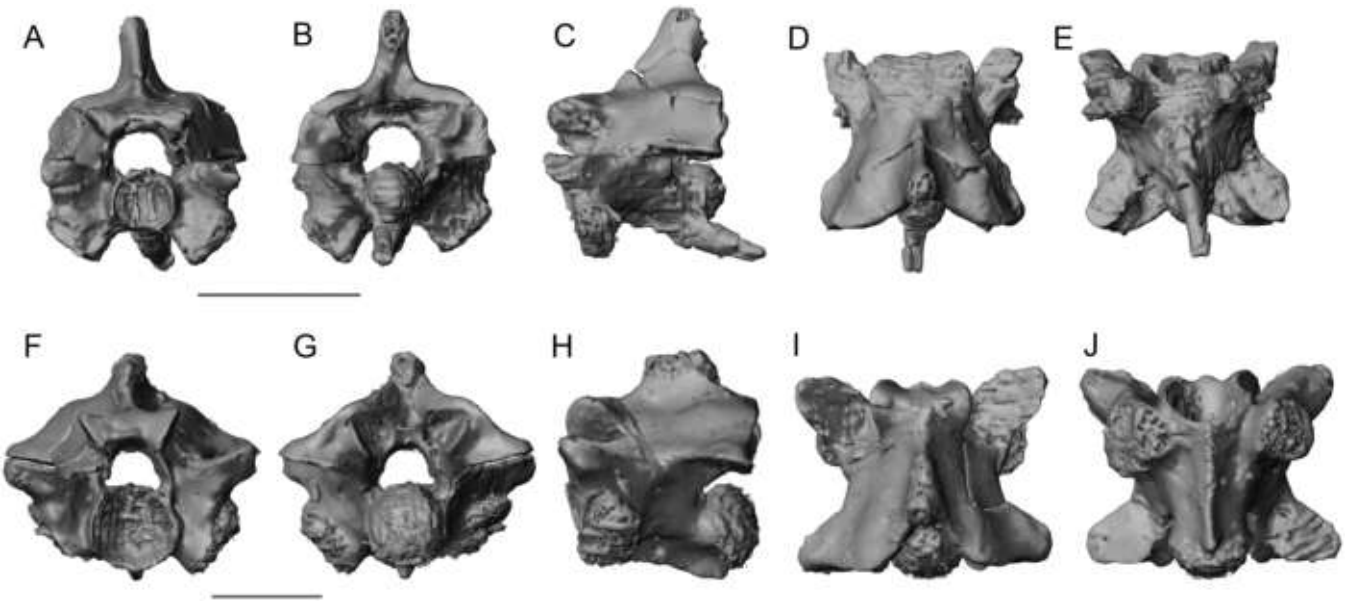

Figure 10. *Eoconstrictor barnesi*, GMH LIX-3-1992, paratype, digital renderings of the segmented precloacal vertebrae. A–E, anterior precloacal in anterior (A), posterior (B), left lateral (C), dorsal (D), and ventral (E) view; (F–J) middle precloacal in anterior (F), posterior (G), left lateral (H), dorsal (I), and ventral (J) view.

of the two elements (Figs 3B, 5A–C). It is fairly robust, slightly arched in lateral view and mostly straight in dorsal view, except towards its anterior end, where it bends medially to a small degree. A relatively small mental foramen is located ventral to the fourth tooth position. There is a distinct posterodorsal ramus, deeper and twice the length of the posteroventral ramus. The two rami are separated by a deep notch where the surangular process of the compound bone articulates. The Meckelian groove is shallow, runs along the ventral margin of the dentary and extends anteriorly to its far end. The dentary bears 18 tooth positions.

The compound bone (Fig. 5E–G) is slightly longer than the dentary and bears a prominent rounded coronoid process with an anterior margin that forms almost a 90° angle with the straight dorsal margin of the surangular process. At the base of the coronoid process, where this meets the surangular process, lies the anterior surangular foramen. A tall surangular crest slopes posteroventrally from the coronoid process and delimits the adductor fossa laterally. The prearticular crest is somewhat damaged, but appears to be much lower than the surangular crest. Posteriorly, the mandibular cotyle is delimited anteriorly by a distinct transverse crest, which laterally merges with the crest for the insertion of the m. adductor externus superficialis. This latter crest slopes anteroventrally from its position near the cotyle until it approaches the ventral margin of the compound bone halfway toward the coronoid process, then gently rises again until it reaches a point ventral to the coronoid process.

The left splenial is preserved and appears to be missing only its most posterodorsal portion (Fig. 5D, H). It is an elongate, subtriangular element, with a distinct longitudinal medial keel that fits into the Meckelian groove. A foramen for the anterior intermandibularis nerve is only partially preserved, the portion of the bone framing the foramen dorsally being lost due to breakage. The articular surface for the angular is only partially preserved (dorsal portion missing).

The left coronoid is complete, and has a distinct hockey-stick shape, with a strap-like ascending process expanding anteroventrally into a broader, mediolaterally flat anteroventral portion (Fig. 5I, J). The angle between the posterior ascending ramus and the horizontal portion is about 120°.

Postcranial material of GMH XXXVIII-20-1964 (holotype)

The postcranial skeleton of this specimen is partially disarticulated into a series of segments, but a large part of the body is preserved, with the exception of the most anterior precloacal, the cloacal, and most of the caudal regions. Only about 10 distal caudal vertebrae remain (Fig. 2; Supporting Information, File S1: Fig. S1). This snake has at least 189 vertebrae preserved, but if we consider that the most anterior elements, the cloacal region, and most of the tail are missing (and possibly also the posterior end of the precloacal series), then the total number of vertebrae must have been much higher. In fact, the number of precloacal vertebrae in specimens of *E. fischeri* varies between 246 and 303 (see Remarks above), so it is plausible that *E. barnesi* had a similar number, with some variability among individuals.

The average centrum length of the largest vertebrae in GMH XXXVIII-20-1964 is 12.8 mm, and the vaulting ratio (*sensu* Georgalis *et al.* 2021) is 0.33 (averages from 4 among the largest mid-trunk vertebrae).

The overall vertebral morphology of this specimen is mostly consistent with that observed in members of Boidae (see Szyndlar and Georgalis 2023). The anterior trunk vertebrae have distinct hypapophyses that decrease in height posteriorly and eventually turn into low but distinct haemal keels on the mid-trunk vertebrae. Posteriorly in the trunk region, the haemal keel grades into a gently rounded surface with a small posteroventral tubercle. The most posterior precloacal vertebrae have a very narrow, mediolaterally compressed, mid-sagittal portion of the centrum that is delimited laterally by deep subcentral fossae. There are only 10 posterior caudal vertebrae that can be

confidently identified, four preserved in dorsal view and six in left lateral view (Fig. 2; Supporting Information, File S1: Fig. S1). These vertebrae are anteroposteriorly elongate, bear low neural spines, small but distinct prezygapophyseal accessory processes, and well-developed subtriangular haemapophyses that point posteroventrally.

All vertebrae possess a pair of small subcentral foramina, at least in all those where this feature can be ascertained. The neural spines of the mid-trunk vertebrae are trapezoidal in lateral view, dorsally flat and with an anterior edge that is well posterior to the zygosphene roof. Posteriorly they slightly overhang the condyle, which is robust and hemispherical and otherwise exposed in dorsal view in disarticulated vertebrae. Prezygapophyseal accessory processes can be observed in all of the preserved regions of the body. Parasagittal ridges *sensu* Hsiou *et al.* (2014) are present on the most robust mid-trunk vertebrae, and at their posterior end sometimes is a small, rounded tubercle, likely marking the insertion of a tendon from the transversospinalis muscle complex.

The zygosphene on mid-trunk vertebrae is relatively thin (width to height ratio = 3.2, where width is measured between the dorsolateral corners of the zygosphene and height is measured in the middle of the zygosphene) and bears a median tubercle. The median tubercle is subtriangular in dorsal view and dorsoventrally thin (lamellar). The anterior margin of the zygosphene is almost straight (excluding lateral projections).

Based on microCT scan images, paracotylar foramina appear to be present on at least some of the vertebrae, but due to the small size of the foramina and the numerous fractures affecting most of the vertebrae it is unclear how frequent this feature is across the vertebral column. Note that paracotylar foramina are present in some (but not all) members of Boidae (see Szyndlar and Georgalis 2023).

The ribs are distinctly curved, with a posterodorsal tubercle and a small foramen on the shaft distal to the articular head.

Cranial material of GMH LIX-3-1992 (paratype)

The skull of this specimen is well preserved albeit not complete (Fig. 6B). Most bones could be segmented from the microCT scan data and visualized digitally in three dimensions (Figs 7, 8). The premaxilla, basioccipital, supraoccipital, otoccipitals, parabasisphenoid, right prootic, vomers, septomaxillae, right maxilla, and right palatine are absent or too fragmentary to be digitally isolated.

Both nasals are partially preserved in this specimen (Fig. 8A–C). The dorsal horizontal lamina is best preserved in the right nasal and has a triangular shape. The descending flange of the nasals is deeper anteroventrally. There is no indication of a process that may have contacted the frontals posteroventrally, and the contact must have been exclusively posterodorsal.

Both prefrontals are preserved (Fig. 7), but the left element is somewhat better preserved (Fig. 8D–F). The prefrontal bears a broad subtriangular lateral lamina, which extends dorsally into a tongue-shaped dorsomedial lappet. The well-developed medial and lateral foot processes delimit a lacrimal foramen that is open ventrally.

Both frontals are present in this specimen, and preserved only slightly offset relative to one another (Fig. 8G–K). In dorsal view they have a subrectangular to trapezoidal outline with a flat dorsal surface. Anteromedially they bear a protruding process for articulation with the nasals. Ventrally the frontals are in contact to fully enclose the space for the olfactory bulbs. Distinct frontal medial pillars are present and meet the lateral flanges to fully enclose the olfactory tracts (Fig. 8I). In lateral view articular facets for the prefrontals and parietal are visible anteriorly and posterodorsally, respectively. The frontals are much deeper posteriorly, where they articulated with the missing parabasisphenoid.

The parietal is very well preserved (Fig. 8L–O). Anteriorly it bears a U-shaped sutural margin for the frontals and has greatly expanded anterolateral processes for articulation with the jugals (*sensu* Palci and Caldwell 2013), which unfortunately are not preserved in this specimen (note that there is some disagreement about the presence of jugals in modern snakes, with the elements in this position behind the orbit interpreted as postfrontals by Zaher *et al.* (2023); however, see Segall *et al.* (2023). In dorsal view the parietal tapers posteriorly forming an almost triangular outline. A distinct mid-sagittal crest is present on the dorsal surface and extends along the posterior half of the bone. In the anterior half the crest is replaced by a low ridge, which appears to extend anteriorly up to the fronto-parietal suture; however, this could be artifactual because the feature is not observed in the holotype (GMH XXXVIII-20-1964) and the anterior region of the parietal presents some fractures.

Both left and right supratemporals are preserved, with the former in slightly better condition (Fig. 8P, Q). In dorsal view the supratemporals are slightly curved, with the concavity facing dorsomedially. The supratemporals are flattened and expanded anteriorly, where they articulate with the prootic and parietal, and taper and thicken posteriorly. The anterior margin of the better preserved supratemporal is gently rounded. A distinct broad facet for articulation with the dorsal condyle of the quadrate is present posterolaterally.

The left prootic is fairly well preserved (Fig. 8R). This bone shows the two openings for the exit of the maxillary (V2) and mandibular (V3) divisions of the trigeminal nerve, separated by a laterosphenoid ossification ('ophidiosphenoid' *sensu* Gauthier *et al.* 2012). The opening for cranial nerve V3 has a rounded anterior margin, unlike that of *E. spinifer* and *E. fischeri*, where the margin of the foramen is pointed anteriorly (Georgalis *et al.* 2021). The opening for the maxillary branch is not closed by the prootic anteriorly but by the parietal. A foramen for the exit of the hyomandibular branch of the facial nerve (cranial nerve VII) is visible just posterior to the exit of the mandibular branch of the trigeminal. Just ventral to this exit is a foramen for the palatine branch of the facial nerve. Foramina for the exit and re-entry of the nerve that innervates the constrictor internus dorsalis muscle complex ('cid nerve' of Rieppel 1979) are visible along the anteroventral margin of the prootic. This margin slopes anterodorsally and forms the sutural contact with the missing parabasisphenoid. Posteroventrally the margin of the prootic slopes at a 45° angle and dorsally forms the anterior margin of the fenestra ovalis in a distinct crista prootica (part of the crista circumfenestralis). The dorsal margin of the prootic is subhorizontal and posterodorsally a shallow excavation marks the articular surface for the supratemporal.

Both left and right quadrates are preserved (Fig. 7), but the left quadrate is fractured at the middle of the shaft, and the two halves are slightly displaced relative to one another. The right quadrate is preserved in much better condition (Fig. 8S–T). In lateral view, the right quadrate has a narrow, subtriangular outline, with a straight anterior margin and a short dorsal margin that slants posteroventrally. In posterior view the bone is constricted mediolaterally just above the ventral condyle, which is distinctly expanded and has a saddle-shaped articular surface for the compound bone. There is no clear indication of the presence of a stylohyal process, but this could be because of poor preservation and/or scan resolution.

The left maxilla is well preserved (Fig. 8U–X). It is an elongate bone (length to height ratio = 7.9) bearing 16 tooth positions, but only seven teeth are preserved in position. There is no facial process, and the maxilla simply increases in depth anteriorly quite gently. In dorsal view an anterior superior alveolar foramen is clearly visible above the third tooth position. Three distinct foramina are present medial, anterior, and posterior to the palatine process. The anterior foramen (variably present in snakes) is here interpreted as the exit of a nerve and/or blood vessel, whereas the other two foramina are for the entry in the maxilla of branches of the maxillary division of the trigeminal nerve (cranial nerve V2). The palatine process is almost triangular in dorsal view, with a long anteromedial edge. Laterally the maxilla bears a single labial foramen located above the fourth tooth position. The ventral margin of the maxilla is straight. In dorsal and ventral views, the anterior end of the maxilla is gently bowed medially. There is no distinct ectopterygoid process, but a thin medial shelf extends along the posterior quarter of the bone.

Both palatines are preserved, but the right element is very badly crushed and could not be segmented. The left palatine, on the other hand, is nearly complete (Fig. 8Y, Z, A'). The palatine lacks a foramen for the suborbital branch of the maxillary division of the trigeminal nerve and appears to have a short and thin choanal process. This could be due to poor preservation, and part of the process may be missing, but the same condition is also observed in the holotype. The anterior edge of the choanal process merges with the dorsal surface of the palatine along a thin crest. The maxillary process is complete, subrectangular in dorsal view, and slightly bent posterolaterally. There are six tooth positions. In lateral view the palatine is deeper at the level of the maxillary process, and its dorsal margin slopes down anteriorly and posteriorly from that point.

The ectopterygoid could be identified only on the left side (Fig. 8B'). It is a flat, V-shaped bone, with distinct medial and lateral processes for articulation with the maxilla. The medial process is much broader than the lateral one and convex in shape. The notch separating the two processes is likely artifactual. The posterior end of the bone is damaged and a surface for articulation with the pterygoid cannot be recognized.

Although both pterygoids are preserved, they lie on top of each other, which complicates the interpretation of their morphology (Fig. 8C'). The right pterygoid is the better preserved of the two. While an accurate tooth count is difficult to obtain on the right pterygoid due to the numerous fractures in this element, 11 tooth positions can be identified on the left pterygoid. The dentigerous portion is fairly straight, whereas the quadrate ramus arches posterolaterally, is blade-like in shape and has a distinct longitudinal groove for the attachment of the musculus (m.) protractor pterygoidei. A distinct and stout ectopterygoid process is present lateral to the posterior half of the tooth row; this process has a broad medial base and tapers into a laterally facing sub-elliptical articular facet for the ectopterygoid.

Lower jaw of GMH LIX-3-1992 (paratype)

The left lower jaw of this specimen is very well preserved (Figs 6, 7). The left dentary (Fig. 9A–C) is a robust element that bears 17 tooth positions, with 11 teeth still in place. In dorsal view this bone is broader posteriorly than anteriorly and is gently curved mediolaterally. A single mental foramen is present ventral to the fourth tooth position. The posterodorsal ramus of the dentary is deeper and about twice the length of the posteroventral ramus. In medial view, a shallow Meckelian groove extends all the way from the posterior notch between posterodorsal and posteroventral rami to the anterior end of the dentary. A medial subdental shelf is absent.

The compound bone (Fig. 9D–F) is slightly longer than the dentary and bears a distinct surangular process that fits between the posterodorsal and posteroventral rami of the latter bone. The dorsal margin of the surangular process slopes posterodorsally into a distinct coronoid process. Anteroventral to this process, in lateral view, an anterior surangular foramen is visible. The adductor fossa is deep, well defined, and bordered medially and laterally by the prearticular and surangular crests, respectively. These crests are subequal in height. The mandibular cotyle is slightly offset laterally relative to the rest of the compound bone, because of a gentle bend in the posterior quarter of this bone (this offset is absent in *E. fischeri*, where the cotyle is in line with the main body of the compound). A distinct mediolateral crest marks the anterior margin of the mandibular cotyle. There is effectively no retroarticular process, but a blunt ending of the compound posterior to the cotyle. The ventral margin of the compound bone is relatively straight, with only a gentle sigmoidal curvature. Along the ventrolateral margin of the compound bone is a longitudinal crest, presumably for the insertion of the m. adductor externus superficialis (Fig. 9E). This crest starts anteriorly in the middle of the ventral margin of the compound and extends posteriorly up to the anterior margin of the mandibular cotyle.

The splenial and angular are not preserved on the left side, but fortunately their right counterparts are (Fig. 9G–H). The right angular is complete, while the right splenial is missing the most anterior portion, but is preserved well enough that most details are visible. The intramandibular joint is clearly visible between the angular and the splenial, with a convex surface on the former fitting into a concave facet on the latter. Both elements are subtriangular, although the angular is much deeper at mid-length and slightly longer anteroposteriorly. A foramen for the exit of a branch of the intermandibularis nerve is visible on each element (i.e. anterior and posterior mylohyoid foramina).

The left coronoid is well preserved, although a small portion of its anteroventral end may be missing due to breakage (Fig. 9I, J). This element is comma shaped and strap like and articulates with the medial side of the well-developed coronoid process on the compound. Both the coronoid bone and the coronoid process of the compound are subequal in height when articulated.

Postcranial material of GMH LIX-3-1992 (paratype)

The postcranium of this specimen is preserved almost in articulation, with very little distortion and displacement (Fig. 6A). Only the cloacal and caudal regions cannot be identified. There are at least 113 preserved precloacal vertebrae. The largest mid-trunk vertebrae are 10.8 mm long (average centrum length of four among the largest mid-trunk vertebrae).

As in the holotype described above, the vertebral morphology of the paratype is consistent with that of Boidae (see Szyndlar and Georgalis 2023). The anterior precloacals have long and slender hypapophyses, strongly projecting posteriorly, and equally long neural spines (Fig. 10). Their synapophyses project ventrally below the ventral margin of the small and subcircular cotyle. The mid-trunk vertebrae (Fig. 10F–J) lack hypapophyses, but have a distinct mid-sagittal keel; the midventral keel disappears in the most posterior precloacals (Fig. 6C). The 'vaulting ratio' (*sensu* Georgalis *et al.* 2021) of the two segmented vertebrae is 0.55 for the anterior precloacal (Fig. 10A–E) and 0.32 for the mid-trunk vertebra (Fig. 10F–J). The centra are robust, subtriangular in shape, and bear a pair of small subcentral foramina, features that are similar to those of other booids. The condyles are robust and hemispherical, exposed in dorsal view in disarticulated vertebrae. The neural spines are anteroposteriorly short with the anterior edge well posterior to the zygosphene roof. In lateral view the neural spines are trapezoidal, with a slanting anterior margin and a straight dorsal margin. Parasagittal ridges (*sensu* Hsiou *et al.* 2014) are present on the most robust mid-trunk vertebrae. Distinct small prezygapophyseal accessory processes are consistently present on all precloacal vertebrae. In dorsal view the anterior margin of the zygosphene is almost straight (excluding lateral projections) and is marked by the presence of a distinct sub-triangular median tubercle. The tubercle is broad mediolaterally at its base, but fairly thin dorsoventrally (lamellar tubercle *sensu* Georgalis *et al.* 2021). The zygosphene of the mid-trunk vertebrae is relatively thin (width to height ratio = 3.5). The two vertebrae that were segmented both have small paracotylar foramina (Supporting Information, File S1: Fig. S2).

The ribs are typical for alethinophidians, well curved, with a posterodorsal tubercle and a small foramen on the shaft just distal to the articular head.

Phylogenetic results

Although our analysis included sampling across all snakes, we will focus our description of the results on the relationships within booids and close relatives, for sake of clarity and brevity.

Bayesian analyses

Dataset I: The Bayesian analysis of the morphological dataset did not retrieve the clade Constrictores [*sensu* Georgalis and Smith (2020) here and throughout the manuscript], as Caenophidia are nested within the larger clade inclusive of boas and pythons (Supporting Information, File S1: Fig. S4). Here taxa traditionally assigned to Pythonoidea form successive sister taxa/clades leading to Caenophidia. *Messelopython* Zaher & Smith, 2020, is reconstructed as a stem taxon to the large clade that includes traditional members of Booidea and Caenophidia, where only the latter group is monophyletic. *Eoconstrictor* was retrieved in a clade inclusive of members traditionally assigned to Boidae (non-monophyletic), *Candoia carinata* (Schneider, 1801), *Sanzinia madagascariensis* (Duméril & Bibron, 1844), and *Acrantophis madagascariensis* (Duméril & Bibron, 1844).

Messelophis Baszio, 2004 and *Rieppelophis* Scanferla, Smith & Schaal, 2016 form a well-supported clade (posterior probability PP = 0.95) that is sister to a large clade inclusive of *Calabaria reinhardtii* (Schlegel, 1851), the 'old' traditional concept of Erycidae (which would practically correspond to the distinct lineages Erycidae plus Charinainae in Pyron *et al.* (2014), a grouping also informally called 'erycines' in Smith and Georgalis (2022): *Charina bottae* (Blainville, 1835), *Lichanura trivirgata* Cope, 1861a, *Eryx johnii* (Russell, 1801), and the recently described fossil form *Rageryx* Smith & Scanferla, 2021), Ungaliophiinae, *Tropidophis haetianus* (Cope, 1879), *Casarea dussumieri* (Schlegel, 1837), and Caenophidia (Supporting Information, File S1: Fig. S4).

The posterior probabilities (PP) for some of the nodes in this tree are relatively low (< 0.5) and therefore the support for the overall topology is weak; however, the placement of *E. barnesi* as the sister taxon to *E. spinifer* is somewhat better supported (PP = 0.69).

Dataset II: The Bayesian analysis of the combined data (morphology and molecules) retrieved a monophyletic Constrictores, which consists of the two major clades Pythonoidea and Booidea, and is the sister group to a clade inclusive of *Casarea* Gray, 1842 and Caenophidia (Fig. 11A). Of note is that *Casarea*, a representative of Bolyeriidae, is here not part of Constrictores, unlike in Georgalis and Smith's (2020) reference phylogeny.

According to this topology the most basal members of Booidea appear to be the Sanziniidae, followed by a clade inclusive of *Messelophis* and *Rieppelophis*. As in other recent phylogenies, the traditional clade Erycidae is not recovered, and its constituent taxa are separated in different clades/lineages above *Calabaria* Gray, 1858: Charinaidae and a separate clade inclusive of *Eryx* Daudin, 1803, and *Rageryx*. These clades are followed crownward by *Candoia* Gray, 1842, a clade inclusive of the three species of *Eoconstrictor*, and a clade inclusive of Neotropical boas [i.e. *Boa constrictor* Linnaeus, 1758, *Chilabothrus angulifer* (Cocteau and Bibron 1843), *Corallus caninus* (Linnaeus, 1758), *Eunectes murinus* (Linnaeus, 1758), and *Epicrates cenchria* (Linnaeus, 1758)].

Within Booidea, branch support is relatively weak (PP < 0.5) for the placement of *Calabaria*, Charinaidae, *E. fischeri*, and for the placement of *Eoconstrictor* as a stem member of Boidae; however, the positioning of *Eoconstrictor* within a clade inclusive of *Candoia*, Neotropical boas, *Eryx*, and *Rageryx* is moderately supported (PP = 0.84).

Parsimony analyses

Dataset I: The parsimony analysis of the morphological dataset (Dataset I; 52 taxa, 240 unordered characters) retrieved 102 most parsimonious trees (MPTs) of 947 steps (consistency index CI = 0.33; retention index RI = 0.66). The strict consensus of these trees is not well resolved, and only major clades such as crown snakes and Caenophidia are retrieved (Supporting Information, File S1: Fig. S5). Importantly, however, the three species of *Eoconstrictor* formed a clade in all MPTs. The majority-rule consensus tree (MRCT) is fully resolved (Supporting Information, File S2). In this topology, Pythonidae form a clade

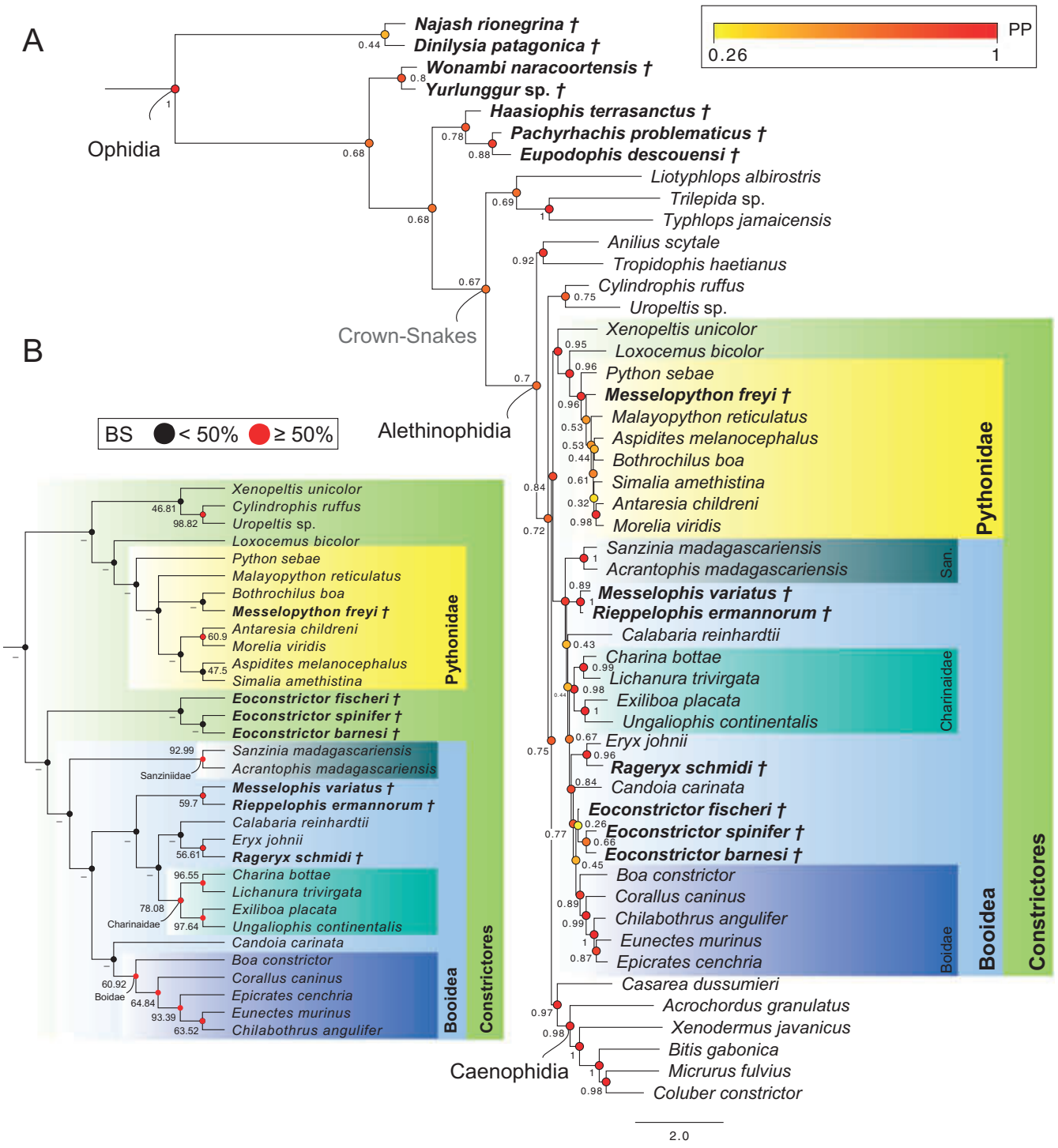

Figure 11. Phylogenetic position of *E. barnesi* (GMH XXXVIII-20-1964 and GMH LIX-3-1992 merged) within snakes obtained from Bayesian inference analysis (A) and parsimony analysis (B) of the combined morphological and molecular data (Dataset II). PP denotes posterior probability and BS denotes bootstrap support. The strict consensus tree in (B) is derived from the two most parsimonious trees of 21,543 steps each (CI = 0.51; RI = 0.37). Bold names in the topology denote fossil species.

with *Messelopython* at the base [as was envisaged by Smith and Scanferla (2022) who named the group Messelopythonidae], and these form the sister group to a large clade inclusive of members of Booidea (non-monophyletic) and Caenophidia. This large clade is in turn subdivided into two large sub-clades: one where *Messelophis*, *Rieppelophis*, and *Eoconstrictor* are together with Neotropical boas, *Candoia*, *Acrantophis* Jan, 1860 in Jan and Sordelli 1860–1866, and *Sanzinia* Gray, 1849; and the other consisting of *Eryx*, *Rageryx*, *Calabaria*, *Charina* Gray, 1849, *Lichanura* Cope, 1861a, *Tropidophis* Cocteau & Bibron, 1843, *Casarea*, and Caenophidia. Ungaliophiinae are placed as sister to a clade inclusive of *Tropidophis*, *Casarea*, and Caenophidia, and the traditional concept of Erycidae was not recovered.

The bootstrap support (BS) values for these clades are all relatively low (BS < 60), with the exception of Caenophidia (BS = 81) and the clade formed by *Messelophis* and *Rieppelophis* (BS = 74) (Supporting Information, File S1: Fig. S5).

Dataset II: The parsimony analysis of the combined dataset (molecular plus morphological data; Dataset II) retrieved two MPTs of 21,543 steps (CI = 0.51; RI = 0.37). The strict consensus (Fig. 11B; Supporting Information, File S1: Fig. S6) is mostly resolved and while it retrieves a monophyletic Constrictores, the latter besides including booids and pythonoids also includes some unorthodox taxa such as *Uropeltis* Cuvier, 1829 and *Cylindrophis* Wagler, 1828 as members of Pythonoidea (the clade normally inclusive only of Pythonidae, *Xenopeltis* Reinwardt 1827 (in Boié 1827), *Loxocemus* Cope, 1861b, and the extinct family Messelopythonidae). However, support for the placement of *Cylindrophis* and *Uropeltis* in a sister group to *Xenopeltis* is low (BS = 47). This expanded Pythonoidea is the sister group of another large clade inclusive of *Eoconstrictor* (all three species in a clade) and crown Booidea (i.e. *Eoconstrictor* is a stem booid). Sanziniidae is recovered as the earliest-branching crown booid clade and forms the sister group of a large clade that consists of two sub-clades: Boidae and *Candoia* on one side, and Charinaidae, *Calabaria*, *Eryx*, *Rageryx*, *Messelophis*, and *Rieppelophis* on the other. *Messelophis* and *Rieppelophis* form a clade together at the base of this second sub-clade, while *Rageryx* was recovered as the sister taxon to *Eryx*.

The relationships within Pythonoidea are not strongly supported, and while *Messelopython* is placed as a sister taxon to *Bothrochilus boa* (Schlegel, 1837), this clade is in a polytomy with *Malayopython reticulatus* (Schneider, 1801) and a second clade inclusive of *Antaresia childreni* (Gray, 1842), *Morelia viridis* (Schlegel, 1872), *Aspidites melanocephalus* (Krefft, 1864), and *Simalia amethistina* (Schneider, 1801).

The bootstrap support values for clades within Pythonoidea are generally low (BS < 50), and the highest value is for the node at the base of the clade inclusive of *Antaresia* Wells & Wellington, 1984, and *Morelia* Gray, 1842 (BS = 61). The support for *Eoconstrictor* at the base of Booidea is also low (BS < 50) (Fig. 11B; Supporting Information, File S1: Fig. S6).

Most nodes within Booidea have moderate (~60) to very good (> 90) bootstrap support, with the exceptions of *Candoia* as a sister to Boidae, and the nodes at the base of the subclade sister to *Candoia* plus Boidae. The support for the nodes at the base of Booidea is not strong either (nodes not retrieved in bootstrap consensus tree).

Charinaidae is moderately well supported (BS = 78), and the sister group relationships of *Exiliboa placata* Bogert, 1968, with *Ungaliophis continentalis* Müller, 1880 (i.e. Ungaliophiinae) and of *Charina* with *Lichanura* (i.e. Charinainae) are both strongly supported (BS = 98 and BS = 97, respectively).

Additional analyses

The results from the same set of analyses (Bayesian and parsimony, Dataset I and Dataset II) where multistate morphocline characters were ordered produced results that are consistent with those described above, but generally with lower resolution (Supporting Information, File S2).

We also ran unordered Bayesian and parsimony analyses of Dataset II where the two specimens of *E. barnesi* were scored separately and where two additional very fragmentary taxa from North America were included: the early snake *Coniophis precedens* from the Late Cretaceous and *Boavus occidentalis* from the Eocene. The Bayesian analysis retrieved *Messelophis* and *Rieppelophis* as sister taxa (PP = 0.99) and forming a clade with Sanziniidae at the base of Booidea (PP = 0.24); and this clade was followed crownward within Booidea by *Calabaria*, Charinaidae, *Boavus* Marsh, 1871, Erycidae s.l. (i.e. *Eryx* and *Rageryx*; PP = 0.86), *Candoia*, *Eoconstrictor* (i.e. all three species, and with the two specimens of *E. barnesi* as sister OTUs; PP = 0.48 for the whole *Eoconstrictor* clade, and PP = 0.92 for the two specimens of *E. barnesi* as sister OTUs), and Boidae (PP = 0.81). The support for the node joining *Eoconstrictor* to Boidae was low (PP = 0.34). Support was low also for the placement of *Boavus* (PP = 0.36). *Messelopython* was found to be a basal member of Pythonidae just above *Python sebae*, but again with low support (PP = 0.31) (Supporting Information, File S1: Fig. S7; File S2).

The strict consensus tree resulting from the parsimony analysis of this expanded data set was very poorly resolved, and all of the fossil taxa fell in a large polytomy within Constrictores, except for *Messelophis* and *Rieppelophis* which were still retrieved as sister taxa (Supporting Information, File S2). The MRCT was much better resolved, and consistent with the main results: *Messelophis* and *Rieppelophis* forming a clade at the base of Booidea (70%); *Eoconstrictor* still at the base of Boidae plus *Candoia* (24%); *Coniophis* Marsh, 1892, as sister taxon to *Anilius scytale* (Linnaeus, 1758) at the base of the snake radiation (96%); the two specimens of *E. barnesi* as sister OTUs (96%) and in a clade with *E. spinifer* and *E. fischeri* (25%); and *Boavus* as the sister taxon to a clade inclusive of Charinaidae, *Calabaria*, *Eryx*, and *Rageryx* (29%); and *Messelopython* as sister to *Bothrochilus* Fitzinger, 1843 (80%) within Pythonidae (Supporting Information, File S2).

For a list of synapomorphies retrieved in the Bayesian and Parsimony analyses of the combined dataset (Dataset II) see Supporting Information, File S1: Table S2.

Character optimization on preferred topology

The phylogenetic relationships that we focus on are those obtained from the Bayesian analysis of the combined dataset (Dataset II) with 52 taxa, where *Eoconstrictor* was retrieved as a stem boid (Fig. 11A). The parsimony analysis placed *Eoconstrictor* as a stem booid (Fig. 11B), and although we think this may be plausible, we still prefer the result from the Bayesian analysis because of its more refined approach in the analysis of molecular data (e.g. data partitioning, modelling of changes for third codon positions and transitions vs. transversions, all of which are not modelled by the parsimony optimality criterion), which led to more orthodox relationships among extant taxa (e.g. uropeltids).

Based on character optimization performed on the Bayesian topology the derived anatomical features shared by *Eoconstrictor*, *Eoconstrictor* + Boidae, and Boidae are shown in Supporting Information, File S1: Table S2. As discussed above we prefer the results of the Bayesian analysis; however, for sake of completeness we also present the synapomorphies supporting the possibility that *Eoconstrictor* may be a stem booid, as suggested by our combined evidence parsimony analysis (Fig. 11B). For a list of synapomorphies retrieved in the parsimony analysis of Dataset II that support the clades *Eoconstrictor* + Booidea, and Booidea see Supporting Information, File S1: Table S3.

DISCUSSION

The two specimens are very similar and referrable to a single species, despite minor differences which are potentially ontogenetic. The holotype GMH XXXVIII-20-1964 differs from the paratype GMH LIX-3-1992 in the following features: the dorsal margin of the maxilla (straight in GMH LIX-3-1992 vs. sigmoid in GMH XXXVIII-20-1964), frontoparietal suture (U-shaped in GMH LIX-3-1992 vs. gently concave in GMH XXXVIII-20-1964), shape of the frontals in dorsal view (narrow and subrectangular in GMH LIX-3-1992 vs. semicircular in GMH XXXVIII-20-1964), shape of the coronoid process (low in GMH LIX-3-1992 vs. tall in GMH XXXVIII-20-1964), height of the surangular crest relative to the prearticular crest (crests subequal in height in GMH LIX-3-1992, surangular crest taller in GMH XXXVIII-20-1964), and tooth counts (see Table 1). We believe that all of these differences can be potentially attributed to ontogeny (GMH

Table 1. Summary table comparing the two fossil specimens of *E. barnesi* (GMH XXXXVIII-20-1964 and GMH LIX-3-1992) with other Constrictores with known cranial material from the Eocene of Europe. Tooth counts for *E. fischeri* are based on specimen SMF-ME 11 398, but Scanferla and Smith (2020a) report variable numbers of maxillary and dentary teeth in a range of referred specimens (15–18 maxillary and 18–19 dentary). Abbreviations: L, length; H, height; W, width

	Palaeopython cadurcensis	*Eoconstrictor fischeri*	*Eoconstrictor spinifer*	*Phosphoroboa filholii*	GMH XXXXVIII-20-1964	GMH LIX-3-1992
Locality	Phosphorites du Quercy, France	Middle Messel Formation, Germany	Geiseltal, Saxony-Anhalt, Germany	Phosphorites du Quercy, France	Geiseltal, Saxony-Anhalt, Germany	Geiseltal, Saxony-Anhalt, Germany
Age	middle or late Eocene	early to middle Eocene	late early to middle Eocene	middle to late Eocene	late early to middle Eocene	late early to middle Eocene
Number of labial foramina	1	4	1	NA (not preserved)	1	1
Maxilla morphology 1 - dorsal margin	Weakly sigmoid	Sigmoid	Straight	Weakly sigmoid	Sigmoid	Straight
Maxilla morphology 2 - (L/H)	NA (incomplete)	7.22	4.68	NA (incomplete)	7.5	7.9
Frontoparietal suture	NA (not preserved)	U-shaped	NA (poorly preserved)	V-shaped	Straight	U-shaped
Zygosphene - median tubercle	Absent on holotype	Present and triangular	Absent	Present and rounded or absent	Present and triangular	Present and triangular
Zygosphene thickness in mid-trunk vertebrae - (W/H) (~2 = thick; ~3 = thin)	Thick: 2.3 (lectotype, MNHN.F.QU16318)	Thin: 3.5 (holotype, SMF-ME 929)	Thin: 3.6 (paralectotype, GMH Ce I-5822-1926)	Thin: 2.9 (holotype, MNHN.F.QU16322)	Thin: 3.2	Thin: 3.5
Prezygapophyseal accessory processes	Present	Present	Absent in anterior precloacal vertebrae	Present	Present	Present
Coronoid process of compound bone	NA (not preserved)	Low with a pointed anterior apex	NA (not preserved)	NA (not preserved)	Very tall and rounded anteriorly	Low and rounded anteriorly
Position of the mental foramen	Below 4th tooth position	Below 5th tooth position	NA (not preserved)	Below 5th tooth position	Below 4th tooth position	Below 4th tooth position
Frontals - outline in dorsal view	NA (not preserved)	Subrectangular with slightly convex lateral margin	NA (not preserved)	NA (not preserved)	Semicircular	Subrectangular
Number of maxillary teeth	>13 (maxilla incomplete posteriorly)	17	>14 (maxilla incomplete posteriorly)	>12 (maxilla incomplete anteriorly)	17	16
Number of dentary teeth	18	18	NA (not preserved)	>17 (all dentaries incomplete)	18	17
Number of palatine teeth	NA (not preserved)	5	NA (not preserved)	NA (not preserved)	6	6
Number of pterygoid teeth	NA (not preserved)	11	11	14	10	11

XXXVIII-20-1964 is about 35% larger than GMH LIX-3-1992). Tooth counts have been shown to be intraspecifically variable in booids (Kluge 1991, 1993), and our observation of specimens of the boid snake *Eunectes murinus* at different age stages (AMNH R29349, AMNH R54158, AMNH R57474, and ZFMK 5179) as well as images from the literature of juvenile and adult *Boa constrictor* confirm that also the other above-mentioned features can vary during ontogeny (Supporting Information, File S1: Fig. S8; Smith and Scanferla 2016, fig. 3). We thus consider these two specimens as members of the same species, but representing different ontogenetic stages.

GMH XXXVIII-20-1964 (*E. barnesi* holotype) and GMH LIX-3-1992 (*E. barnesi* paratype) could be confidently identified as booids based on general morphology of the skull and vertebrae (assessment confirmed by phylogenetic analyses above), and were thus compared to other geographically and/or temporally close large-bodied fossil snakes (Constrictores), namely *Eoconstrictor fischeri* (Schaal, 2004), *Eoconstrictor spinifer*, *Palaeopython* spp., and *Phosphoroboa filholii* (Rochebrune, 1880), all from the Eocene of Europe, and *Boavus occidentalis* Marsh, 1871, the best preserved booid species from the Eocene of North America (note: *Boavus idelmani* Gilmore, 1938, would be more complete but unfortunately the type specimen is lost).

Smaller fossil booid species, such as *Messelophis variatus* Baszio, 2004, and *Rieppelophis ermannorum* (Schaal & Baszio, 2004) from Messel, are not compared in detail here with the two new specimens from Geiseltal, but suffice it to say that their morphology is very different both cranially and postcranially (see Scanferla *et al.* 2016, Scanferla and Smith 2020b; see also the results of our Bayesian phylogenetic analysis, which places them distant from *Eoconstrictor*, Fig. 11A).

GMH LIX-3-1992 and GMH XXXVIII-20-1964 most closely resemble two fossil species of snakes from the Eocene of Europe: *E. fischeri*, from Messel, and *E. spinifer*, from the same general locality of Geiseltal. Indeed, GMH LIX-3-1992 is morphologically very similar to *E. fischeri*, from the early–middle Eocene of Messel (47 Mya) (for a comparison with other European species see Table 1) but differs in the number of labial foramina in the maxilla (4 vs. 1) and in the position of the mental foramen (below the 5th tooth alveolus in *E. fischeri* vs. below the 4th in GMH LIX-3-1992). We consider these differences enough to differentiate the two at the species level. As for *E. spinifer*, this is known so far with confidence only from its type material, comprising solely of parts of the skull and a few anterior precloacal vertebrae (Georgalis *et al.* 2021). *Eoconstrictor barnesi* can nevertheless be differentiated from *E. spinifer* by a number of cranial and vertebral features (see Diagnosis above).

Georgalis *et al.* (2021) described but did not name a possible member of the genus *Eoconstrictor* in the Geiseltal fossil fauna that is most similar to *E. fischeri* but also different from the co-occurring *E. spinifer*. These authors referred this form to *Eoconstrictor* cf. *fischeri* and found that it represents the most abundant fossil snake in Geiseltal, known by dozens of specimens from multiple quarries (Georgalis *et al.* 2021). However, this form was described based predominantly on postcranial remains and in the single figured specimen that comprised some fragments of the skull (GMH XXXVIII-7-1964; Georgalis *et al.* 2021: fig. 64) these appear to be non-informative for a more precise determination. Nevertheless, the abundant vertebrae of *E.* cf. *fischeri* from Geiseltal described by Georgalis *et al.* (2021) match well in morphology with vertebrae of *E. barnesi* described here. We thus anticipate that many of the specimens that were previously assigned to *E.* cf. *fischeri* could be conspecific with *E. barnesi*, rather than representing an additional distinct congeneric species in the same locality. Finally, another similar form of the same genus, *E.* cf. *fischeri*, has been described from the middle–late Eocene of Dielsdorf, Switzerland by Georgalis and Scheyer (2019). This form, also exclusively known from vertebral material, is possibly more closely related to (or conspecific with) *E. fischeri* from Messel considering the geographic proximity of Dielsdorf to Messel, but only the discovery of its cranial material will shed light on this matter.

Besides *E. spinifer* and *E.* cf. *fischeri*, there is another constrictor species that has been previously recognized from the locality of Geiseltal: *Palaeopython ceciliensis* Barnes, 1927. *Palaeopython ceciliensis* was based on an isolated fragmentary mid-trunk vertebra (GMH CeI-2978-1926) recovered from a single fossil site within the locality of Geiseltal (Cecilie I) (Barnes 1927). However, in addition, a large number of specimens from multiple quarries in Geiseltal has been referred to this species, including also partial skeletons (Kuhn 1939, Georgalis *et al.* 2021). *Eoconstrictor barnesi* can be differentiated from the type of *P. ceciliensis* based on the thickness of the zygosphene (thicker in *P. ceciliensis*, with a width/height ratio of 2.5 vs. a ratio of 3.2–3.5 in the mid-trunk vertebrae of *E. barnesi*), and a median tubercle on the anterior margin of the zygosphene that is absent or only weakly developed in *P. ceciliensis*, whereas it is well developed and subtriangular in dorsal view in *E. barnesi*. A well-preserved mid-trunk vertebra referred to *P. ceciliensis* by Georgalis *et al.* (2021: fig. 20) (GMH LII-37-1971) also appears to be much wider, with an interzygapophyseal constriction ratio (prezygapophyseal width/interzygapophyseal width) of 1.38 vs. 1.75 in the paratype of *E. barnesi*, but the larger specimen (holotype) of *E. barnesi* has a similar ratio at 1.4. Similarly, the other three valid species of the genus *Palaeopython*, i.e. *P. cadurcensis* (Filhol, 1877) from Quercy (France), *P. helveticus* Georgalis & Scheyer, 2019 from Dielsdorf (Switzerland), and *P. schaali* Smith & Scanferla, 2022 from Messel, are distinct enough from the new species in terms of the shape and thickness of the zygosphene and in the absence of a well-developed median tubercle on the anterior margin of the zygosphene (see figs in Georgalis and Scheyer 2019, Georgalis *et al.* 2021, Smith and Scanferla 2022). Moreover, the genus *Palaeopython* has been recently placed in the newly established pythonoid family Messelopythonidae (Smith and Georgalis 2022, Smith and Scanferla 2022), and as such it would only be distantly related to the booid *Eoconstrictor*, which is considered a stem boid (Scanferla and Smith 2020a), a result supported by our preferred phylogenetic analysis (i.e. Bayesian analysis of combined morphological and molecular data).

Although the North American *Boavus occidentalis* from the Green River Formation is the most geographically distant of all reasonably well-known Eocene booids, we consider a comparison important. The two specimens from Geiseltal described here can be readily differentiated from *Boavus* based on vertebral morphology as well as based on the general morphology of the lower jaw. The vertebrae of *B. occidentalis* lack prezygapophyseal accessory processes and a median tubercle on the zygosphene. Furthermore, in *B. occidentalis*, the neural spine rises anteriorly

very close to the anterior edge of the zygosphene, and the anterior precloacals possess a hatchet-shaped hypapophysis, which is a unique feature among booids (Onary *et al.* 2022). The lower jaw of *B. occidentalis* also presents a series of important distinguishing features, namely posterodorsal and posteroventral processes of the dentary that are subequal in length (dorsal process twice as long in the two specimens of *E. barnesi*), a prearticular crest on the compound bone that is considerably taller than the surangular crest (opposite condition in GMH XXXVIII-20-1964 and subequal in height in GMH LIX-3-1992), and a much more strongly developed crest for the insertion of the m. adductor externus superficialis, which protrudes laterally as a distinct flange.

Our phylogenetic analyses employing maximum parsimony and Bayesian inference of a large dataset of snakes inclusive of both morphological and molecular data support a close affinity of the two newly described Geiseltal specimens to *E. fischeri*, regardless of the optimality criterion adopted (i.e. Bayesian vs. parsimony).

Parsimony analysis of the morphological data alone resulted in poorly resolved relationships among extant and fossil booids, but the addition of molecules and adoption of Bayesian analytical methods produced a well-resolved phylogeny, although not all nodes were strongly supported. Combined datasets have previously been shown to be most effective at resolving phylogenetic relationships (Kluge 1989, Pyron 2015, Koch and Parry 2020, Asher and Smith 2021). Thus, we will focus our discussion on the results from the phylogenetic analysis of the combined data (Dataset 2) analysed under Bayesian inference (Fig. 11). This topology supports the monophyly of several families retrieved in previous molecular studies (Pyron *et al.* 2013, Reynolds *et al.* 2014, Burbrink *et al.* 2020).

The fossil snakes from Messel, *Rieppelophis ermannorum* and *Messelophis variatus*, have been previously recovered as the sister-group to the most derived clade Boidae (*sensu* Pyron *et al.* 2014) by Scanferla and Smith (2016), but more recently as part of the radiation of the early diverging Charinaidae, and more particularly Ungaliophiinae (*sensu* Pyron *et al.* 2014) (Scanferla and Smith 2020a), or even in a clade with the North American fragmentary fossil *Boavus occidentalis* (Onary *et al.* 2022). In our study they emerged as a strongly supported clade (PP = 0.96), but their placement within booids is still uncertain and can be affected by simply changing the optimality criterion for the phylogenetic analysis (Fig. 11A, B).

Figure 12. Life reconstruction of *Eoconstrictor barnesi* in the Geiseltal palaeoenvironment, trying to capture a small leptictidan mammal (artwork by Márton Szabó).

The position of the fossil snake *Rageryx* as the sister taxon to *Eryx* is supported in this study (all analyses), but the placement of this clade among booids remains equivocal (Fig. 11; Supporting Information, File S1: Figs S4–S7).

While our study agrees with previous analyses that the fossil snake *Messelopython* is a close relative of Pythonidae (Zaher and Smith 2020, Smith and Georgalis 2022, Smith and Scanferla 2022), we could not find strong support for its exact placement within this clade (Fig. 11; Supporting Information, File S1: Figs S4–S7).

The position of the two new Geiseltal snake specimens in a clade with *E. fischeri* and *E. spinifer* as sister group to the clade Boidae (*sensu* Pyron *et al.* 2014), albeit with low support (PP = 0.45), is consistent with the previous study of Scanferla and Smith (2020a; who recovered *Eoconstrictor* as sister to Boidae with strong support, PP = 0.97). Therefore, the placement of *Eoconstrictor* is more stable compared to that of other fossil booids, because it was recovered as a stem boid in two distinct studies that relied on different and largely independent datasets. This consilience suggests that *Eoconstrictor* could provide a valuable calibration point (minimum age) for the divergence time of crown clade Boidae (*sensu* Pyron *et al.* 2014) from their closest extant sister group. Head (2015) suggested to use the fossil taxon *Titanoboa cerrejonensis* Head *et al.* 2009 from the Palaeocene of Colombia (64–58 Mya) as the calibration point for the split between the clade of Neotropical boas (Boidae *sensu* Pyron *et al.* 2014) and their closest living sister group, considered to be Erycidae in some studies (e.g. Head 2015, Zheng and Wiens 2016) but Candoiidae in others (e.g. Burbrink *et al.* 2020, this study). Nonetheless, despite the potential morphological similarities between *Titanoboa cerrejonensis* and Boidae, the relationships of this fossil taxon still have to be rigorously tested in a phylogenetic analysis of extant and fossil snakes (Head *et al.* 2009, Head 2015). Only the long-anticipated description of the cranial anatomy of *Titanoboa* will eventually shed light on its exact phylogenetic position relative to modern Boidae. In the absence of more robust information about the systematic position of *Titanoboa*, the fossil genus *Eoconstrictor*, and in particular its oldest occurrence, the type species *E. fischeri*, for which a radiometric age is available, would constitute a more robust calibration point (~48 Mya) for the minimum age of the split between crown Boidae and their living sister group.

As a final caveat, we emphasise that the position of *Eoconstrictor* within Alethinophidia (either a stem Boidae or a stem Booidea) remains uncertain, as it can vary with the optimality criterion adopted for phylogenetic analysis (i.e. Bayesian vs. parsimony, respectively). However, an earlier study retrieved boid relationships under both optimality criteria (Scanferla and Smith 2020a), a result consistent with our preferred topology from the Bayesian analysis of Dataset 2. In any case, the possibility that *Eoconstrictor* could be a stem booid cannot be ruled out. Support for the placement of *Eoconstrictor* is unfortunately not strong, mainly as a result of the very fragmentary nature of many fossil booids.

CONCLUSION

The coal deposits of the Konservat-Lagerstätte of Geiseltal, Saxony-Anhalt, Germany, have produced an impressive fossil record of plants and animals, which highlight the rich biota from the paratropical forested palaeoenvironment that existed during the late early or middle Eocene (Lutetian) in Central Europe (Fig. 12) (Franzen 2005, Hastings and Hellmund 2015, Mayr 2020, Ring *et al.* 2020, Georgalis *et al.* 2021). In this study, we described two new exceptionally preserved snakes from Geiseltal, adding to the palaeobiodiversity of this locality as well as to the diversity of fossil booids from the Eocene of Europe. Such diversity of large constrictor snakes is consistent with that found in modern subtropical rainforests (O'Shea 2007).

The specimens GMH XXXVIII-20-1964 and GMH LIX-3-1992 are very similar to *E. fischeri*, but nonetheless morphological differences such as the number of labial foramina of the maxilla and the position of the mental foramen in the lower jaw support the erection of a new distinct species, here named *Eoconstrictor barnesi*; these two snake specimens from Geiseltal also possess a unique combination of morphological features that separates them from the co-occurring *E. spinifer* and other spatiotemporally close genera of constrictors: *Phosphoroboa*, *Palaeopython*, *Messelopython*, *Paleryx*, and *Boavus*.

GMH XXXVIII-20-1964 and GMH LIX-3-1992 slightly differ from each other in features such as the morphology of the frontals, maxilla, and compound bone, but these differences can all be explained by ontogeny if size differences are considered (GMH XXXVIII-20-1964 is about 35% larger), as they are consistent with what can be observed in different ontogenetic stages of modern boids (see Discussion above).

The phylogenetic analyses of the datasets composed of morphology only and combined morphology + DNA data consistently recovered the two snake specimens from Geiseltal in a clade with *E. fischeri* and *E. spinifer* regardless of the optimality criteria adopted. This result corroborates our alpha taxonomic identification and generic assignment. In our preferred topology (Fig. 11A), the clade formed by the three species of *Eoconstrictor* was recovered as sister to Boidae (*sensu* Pyron *et al.* 2014, i.e. neotropical boas), a result that was previously obtained also by Scanferla and Smith (2020a) using an independent dataset.

The consistent placement of the genus *Eoconstrictor* on the stem of the living radiation of Boidae makes it a good candidate to provide a calibration point for the divergence of Boidae from its living sister group in molecular clock studies: the split of Boidae from its living sister group must be at least as old as the most recent common ancestor (MRCA) of Boidae and *Eoconstrictor*, which in turn must be at least as old as the oldest occurrence of *Eoconstrictor* (i.e. 48 Mya).

Our study is consistent with Scanferla and Smith (2020a) in recovering a sister-taxon relationship between booids from the Eocene of Europe and extant South and Central American booids. However, precise palaeogeographic inferences about booids origins and dispersal are hindered by the very poor Palaeogene fossil record of constrictors from Africa (McCartney and Seiffert 2016, Rage *et al.* 2021, Smith and Georgalis 2022) and North America (Holman 2000, Smith 2013, Smith and Georgalis 2022), as well as by the almost total lack of fossil constrictors from Asia throughout the Palaeogene, which is most likely due to collection bias (Georgalis *et al.* 2021, Smith and Georgalis 2022). Nevertheless, several Palaeogene constrictors are indeed known from South America (e.g. Rage 2001, 2008, Head *et al.* 2009), but the precise phylogenetic relationships

of most of them still remain unresolved (Smith and Georgalis 2022). As pointed out previously in Scanferla and Smith (2020a), assuming that the total clade Boidae originated in South America (which, however, rests partly on the assumption that *Titanoboa* is indeed a stem Boidae, see above), it is unclear which dispersal route was followed by early booids to reach Europe. During the Palaeogene, South America was mostly isolated, with only an island arc connecting it to North America, and over a thousand miles of South Atlantic Ocean separating it from Africa (Scotese 2014). However, evidence for dispersal of faunas between South America and Africa in the early Cenozoic has been presented in a previous study (Ezcurra and Agnolín 2012; see also Georgalis *et al.* 2021). The alternative dispersal route would be from South America to Europe via North America at some point during the Palaeocene–Eocene Thermal Maximum (PETM), which does not entail transoceanic dispersal and is supported by evidence from other data sources (McKenna 1983, Krishtalka *et al.* 1987, Augé 2005, Smith 2009, Georgalis and Joyce 2017, Smith and Scanferla 2021), also involving congeneric non-marine reptiles in both North American and European Eocene deposits (Augé 2005, Georgalis and Joyce 2017). However, there is limited overlap between South and North American faunas during the Palaeogene (notable exceptions include caimanine crocodylians; e.g. Walter *et al.* 2021), whereas there is considerable overlap between African and European faunas at that time (e.g. Gheerbrant and Rage 2006, Hipsley *et al.* 2009, Ezcurra and Agnolín 2012, Angst *et al.* 2013, Solé *et al.* 2015, Rabi and Sebők 2015, Pérez García *et al.* 2017, Georgalis *et al.* 2023; see discussion in Georgalis 2021). The poor fossil record of booids from Africa and North America also leaves open the possibility that early stem boids may have originated in one of these two geographic areas, and then dispersed elsewhere from there. The current distribution of fossils is likely heavily influenced by patchy sampling of early booids and future discoveries are required to shed further light on the issue of the origin and dispersal of the early members of this clade.

SUPPLEMENTARY DATA

Supplementary data is available at *Zoological Journal of the Linnean Society* Journal online.

ACKNOWLEDGEMENTS

We thank Michael Stache for his assistance in the Geiseltal Museum and for preparing specimens for CT-scanning. Creation of datasets accessed on MorphoSource was made possible by the following funders and grant numbers: oVert TCN (Open Vertebrate Thematic Collection Network); NSF (National Science Foundation) DBI-1701713; NSF DBI-1701714; NSF DBI-1701769; NSF DBI-1701797; NSF DBI-1701932; NSF DBI-1702263; and the University of Michigan. Creation of datasets accessed on Digimorph.org was made possible by the Deep Scaly Project NSF grant EF-0334961.

A.P. is grateful for assistance provided in collections by: D. Kizirian, R. Pascocello, and M.G. Arnold (American Museum of Natural History); K. Kelly and A. Resetar (Field Museum of Natural History), J.B. Losos, J. Rosado, J. Martinez, and T. Takahashi (Museum of Comparative Zoology); D. Capone, M-A. Binnie, R. Foster, M.N. Hutchinson, and C. Pulka (South Australian Museum); and W. Boehme, P. Wagner, U. Bott, and C. Koch (Zoological Research Museum Alexander Koenig). We are also grateful to M.W. Caldwell and an anonymous reviewer for their helpful comments.

AUTHOR CONTRIBUTIONS

Alessandro Palci (Conceptualization, Methodology, Investigation, Supervision, Project administration, Formal Analysis, Visualization, Writing—original draft, Writing—review & editing, Data curation), Silvio Onary (Formal Analysis, Visualization, Writing—review & editing), Michael S. Y. Lee (Funding acquisition, Formal Analysis, Writing—review & editing), Krister T. Smith (Writing—review & editing), Oliver Wings (Data acquisition, Visualization, Writing—review & editing), Marton Rabi (Conceptualization, Funding acquisition, Writing—review & editing), Georgios L. Georgalis (Writing—review & editing).

CONFLICT OF INTEREST

The authors declare that they have no competing interests.

FUNDING

This study was possible thanks to funding from the Volkswagen Foundation (Az. 90 978 to M.R.), the Coordenação de Aperfeiçoamento de Pessoal de Nível Superior (CAPES Demanda Social to S.O.), Fundação de Amparo à Pesquisa do Estado de São Paulo (FAPESP nos 850 2017/00845-1 and 2019/11166-3 to S.O.), the Ulam Program of the Polish National Agency for Academic Exchange (PPN/ULM/2020/1/00022/U/00001 to G.L.G.), and the Australian Research Council (DP200102328 to M.S.Y.L.).

DATA AVAILABILITY

Files containing the datasets for phylogenetic analysis (morphology, and morphology combined with molecular data) and their scripts are available as Supporting Information, File S2. The microCT scan datasets of GMH XXXVIII-20-1964 and GMH LIX-3-1992 are available on Morphosource.org under the project name 'Eocene snakes from Geiseltal' (https://www.morphosource.org/projects/000541652?locale=en).

REFERENCES

Angst D, Buffetaut E, Lécuyer C *et al.* 'Terror Birds' (Phorusrhacidae) from the Eocene of Europe imply trans-Tethys dispersal. *PLoS One* 2013;**8**:e80357. https://doi.org/10.1371/journal.pone.0080357

Asher RJ, Smith MR. Phylogenetic signal and bias in paleontology. *Systematic Biology* 2021;**71**:986–1008. https://doi.org/10.1093/sysbio/syab072

Auffenberg W. The fossil snakes of Florida. *Tulane Studies in Zoology* 1963;**10**:131–216.

Augé M. Évolution des lézards du Paléogène en Europe. *Mémoires du Muséum National d'Histoire Naturelle, Paris* 2005;**192**:1–369.

Barnes B. Eine eozäne Wirbeltier-Fauna aus der Braunkohle des Geiseltals. *Jahrbuch des Halleschen Verbandes für die Erforschung der mitteldeutschen Bodenschatze, Neue Folge* 1927;**6**:5–24.

Baszio S. *Messelophis variatus* n. gen. nov. sp. from the Eocene of Messel: a tropidopheine snake with affinities to Erycinae (Boidae). *Courier Forschungsinstitut Senckenberg* 2004;**252**:47–66.

de Blainville HMD. Description de quelques espèces de reptiles de la Californie précédée de l'analyse d'un système général d'erpétologie et d'amphibiologie. *Nouvelles Annales du Muséum d'Histoire Naturelle, Paris* 1835;**4**:233–96.

Bogert CM. A new genus and species of dwarf boas from southern Mexico. *American Museum Novitates* 1968;**2354**:1–38.
Boié F. Bemerkungen über Merrem's Versuch eines Systems der Amphibien, Lieferung: Ophidier. *Isis von Oken* 1827;**20**:508–66.
Burbrink FT, Grazziotin FG, Pyron RA *et al.* Interrogating genomic-scale data for Squamata (lizards, snakes, and amphisbaenians) shows no support for key traditional morphological relationships. *Systematic Biology* 2020;**69**:502–20. https://doi.org/10.1093/sysbio/syz062
Cocteau J-T, Bibron G. Reptiles. In: de la Sagra R (ed.), *Historia Física, Política y Natural de la Isla de Cuba*, Vol. **IV**. Paris: Arthus Bertrand, 1843, 1–255.
Cope ED. Contributions to the ophiology of Lower California, Mexico and Central America. *Proceedings of the Academy of Natural Sciences of Philadelphia* 1861a;**13**:292–306.
Cope ED. [Untitled] 'April 9th [...] Some remarks defining [] species of Reptilia Squamata'. *Proceedings of the Academy of Natural Sciences of Philadelphia* 1861b;**1861**:75–7.
Cope ED. Eleventh contribution to the herpetology of tropical America. *Proceedings of the American Philosophical Society* 1879;**18**:261–77.
Cuvier G. *Le Règne Animal Distribué d'Après son Organisation, Pour Servir de Base a l'Histoire Naturelle des Animaux et d'Introduction a l'Anatomie Comparée*, Vol. **5**. Paris: Imprimerie d'Hippolyte Tiliard, 1829.
Daudin FM. *Histoire Naturelle, Générale et Particulière des Reptiles: Ouvrage Faisant Suite à l'Histoire Naturelle Générale et Particulière, Composée par Leclerc de Buffon, et Rédigée par C.S. Sonnini. Tome septième*. Paris: F. Dufart, 1803.
Duméril AHA, Bibron G. *Erpetologie Générale ou Histoire Naturelle Complete des Reptiles*, Vol. **6**. Paris: Librairie Encyclopédique de Roret, 1844.
Ezcurra MD, Agnolín FL. A new global palaeobiogeographical model for the late Mesozoic and early Tertiary. *Systematic Biology* 2012;**61**:553–66. https://doi.org/10.1093/sysbio/syr115
Falk D, Wings O, McNamara M. The skeletal taphonomy of anurans from the Eocene Geiseltal Konservat-Lagerstätte, Germany: insights into the controls on fossil anuran preservation. *Papers in Palaeontology* 2022;**8**:e1453. https://doi.org/10.1002/spp2.1453
Filhol H. Recherches sur les Phosphorites du Quercy Etude des fossiles qu'on y rencontre et specialement des mammiferes Part II. *Annales des Sciences Geologiques* 1877;**8**:1–340.
Fitzinger LJFJ. *Systema Reptilium. Fasciculus primus. Amblyglossae*. Vienna: Braumüller et Seidel, 1843.
Franzen JL. The implications of the numerical dating of the Messel fossil deposit (Eocene, Germany) for mammalian biochronology. *Annales de Paléontologie* 2005;**91**:329–35. https://doi.org/10.1016/j.annpal.2005.04.002
Franzen JL, Haubold H. The biostratigraphic and palaeoecological significance of the Middle Eocene locality Geiseltal near Halle (German Democratic Republic). *Münchner Geowissenschaftliche Abhandlungen* 1987;**10**:93–100.
Georgalis GL. *Necrosaurus or Palaeovaranus*? Appropriate nomenclature and taxonomic content of an enigmatic fossil lizard clade (Squamata). *Annales de Paléontologie* 2017;**103**:293–303. https://doi.org/10.1016/j.annpal.2017.10.001
Gauthier JA, Kearney M, Maisano JA, *et al.* Assembling the squamate tree of life: perspectives from the phenotype and the fossil record. *Bulletin of the Peabody Museum of Natural History* 2012;**53**:3–308. https://doi.org/10.3374/014.053.0101
Georgalis GL. First pan-trionychid turtle (Testudines, Pan-Trionychidae) from the Palaeogene of Africa. *Papers in Palaeontology* 2021;**7**:1919–26. https://doi.org/10.1002/spp2.1372
Georgalis GL, Joyce WG. A review of the fossil record of Old World turtles of the clade *Pan-Trionychidae*. *Bulletin of the Peabody Museum of Natural History* 2017;**58**:115–208. https://doi.org/10.3374/014.058.0106
Georgalis GL, Scheyer TM. A new species of *Palaeopython* (Serpentes) and other extinct squamates from the Eocene of Dielsdorf (Zurich, Switzerland). *Swiss Journal of Geosciences* 2019;**112**:383–417. https://doi.org/10.1007/s00015-019-00341-6
Georgalis GL, Smith KT. Constrictores Oppel, 1811 – the available name for the taxonomic group uniting boas and pythons. *Vertebrate Zoology* 2020;**70**:291–304. https://doi.org/10.26049/VZ70-3-2020-03
Georgalis G, Rabi M, Smith KT. Taxonomic revision of the snakes of the genera *Palaeopython* and *Paleryx* (Serpentes, Constrictores) from the Paleogene of Europe. *Swiss Journal of Palaeontology* 2021;**140**:18. https://doi.org/10.1186/s13358-021-00224-0
Georgalis GL, Prendini E, Roček Z. New information on the Eocene frog *Thaumastosaurus* (Anura, Pyxicephalidae) from the Phosphorites du Quercy, France. *Zoological Journal of the Linnean Society* 2023;**199**:744–70. https://doi.org/10.1093/zoolinnean/zlad047
Gheerbrant E, Rage J-C. Paleobiogeography of Africa: how distinct from Gondwana and Laurasia? *Palaeogeography Palaeoclimatology Palaeoecology* 2006;**241**:224–46. https://doi.org/10.1016/j.palaeo.2006.03.016
Gilmore CW. Fossil snakes of North America. *Geological Society of North America Special Paper* 1938;**9**:1–96.
Gray JE. A synopsis of the genera of Reptilia and Amphibia, with a description of some new species. *Annals of Philosophy, Series 2* 1825;**210**:193–217.
Gray JE. Synopsis of the species of prehensile-tailed snakes, or family Boidae. *Zoological Miscellany* 1842;**2**:41–6.
Gray JE. *Catalogue of the Specimens of Snakes in the Collection of the British Museum*. London: British Museum (Natural History), 1849.
Gray JE. Description of a new genus of Boidae from Old Calabar, and a list of W. African reptiles. *Proceedings of the Zoological Society of London* 1858;**26**:154–67. https://doi.org/10.1111/j.1469-7998.1858.tb06361.x
Hastings AK, Hellmund M. *Gaining Ground: Horse-hunting Crocodiles and Giant Birds: New Research Results on the Eocene World of Germany ca. 45 Million Years Ago*. Halle: Martin-Luther Universität Halle-Wittenberg and Leopoldina Nationale Akademie der Wissenschaften, 2015.
Hastings AK, Hellmund M. Evidence for prey preference partitioning in the middle Eocene high-diversity crocodylian assemblage of the Geiseltal-Fossillagerstätte, Germany utilizing skull shape analysis. *Geological Magazine* 2017;**154**:119–46. https://doi.org/10.1017/s0016756815001041
Haubold H. Zur Kenntnis der Sauria (Lacertilia) aus dem Eozän des Geiseltals. In: Matthes HW, Thaler B (eds), *Eozäne Wirbeltiere des Geiseltales*. Halle: Martin-Luther-Universität Halle-Wittenberg, Wissenschaftliche Beiträge, 1977, 107–112.
Haubold H, Thomae M. Stratigraphische revision der wirbeltierfundstellen des geiseltaleozäns. *Hallesches Jahrbuch für Geowissenschaften* 1990;**15**:3–20.
Head JJ. Fossil calibration dates for molecular phylogenetic analysis of snakes 1: Serpentes, Alethinophidia, Boidae, Pythonidae. *Palaeontologia Electronica* 2015;**18**:1–17.
Head JJ, Bloch JI, Hastings AK *et al.* Giant boid snake from the Paleocene neotropics reveals hotter past equatorial temperatures. *Nature* 2009;**457**:715–7. https://doi.org/10.1038/nature07671
Hellmund M. Letzte Grabungsaktivitäten im südwestlichen Geiseltal bei Halle (Sachsen-Anhalt, Deutschland) in den Jahren 1992 und 1993. *Hercynia* 1997;**30**:163–76.
Hellmund M. The Former Geiseltal Museum (1934-2011), the Eocene Geiseltal Fossillagerstätte (Germany) and the scientific meaning of Ben Barnes as a pioneer of systematic quantitative vertebrate excavations in the Geiseltal Lignites. *Anuário do Instituto de Geociências* 2018;**41**:108–19.
Hipsley CA, Himmelmann L, Metzler D *et al.* Integration of Bayesian molecular clock methods and fossil-based soft bounds reveals Early Cenozoic origin of African lacertid lizards. *BMC Evolutionary Biology* 2009;**9**:151. https://doi.org/10.1186/1471-2148-9-151
Holman JA. *Fossil Snakes of North America: Origin, Evolution, Distribution, Paleoecology*. Bloomington: Indiana University Press, 2000.
Hsiou AS, Albino AM, Medeiros MA *et al.* The oldest Brazilian snakes from the early Late Cretaceous (Cenomanian). *Acta Palaeontologica Polonica* 2014;**59**:635–42.
Hummel K. Schildkröten aus der mitteleozänen Braunkohle des Geiseltales. *Nova Acta Leopoldina* 1935;**2**:457–83.
Jaeger JJ. La faune de Mammifères du Lutétien de Bouxwiller (Bas-Rhin) et sa contribution à l'élaboration de l'échelle des zones biochronologiques de l'Eocène européen. *Bulletin du Service de la*

carte geologique d'Alsace et de Lorraine 1971;**24**:93–105. https://doi.org/10.3406/sgeol.1971.1386
Jan G, Sordelli F. *Iconographie Générale des Ophidiens. Tome premier (livrais 1 à 17), Contenant Cent Deux Planches*. Milan: Georges Jan & Ferdinand Sordelli, 1860–1866.
Kluge AG. A concern for evidence and a phylogenetic hypothesis of relationships among Epicrates (Boidae, Serpentes). *Systematic Biology* 1989;**38**:7–25. https://doi.org/10.1093/sysbio/38.1.7
Kluge AG. Boine snake phylogeny and research cycles. *Miscellaneous Publications Museum of Zoology University of Michigan* 1991;**178**:1–58.
Kluge AG. Aspidites and the phylogeny of pythonine snakes. *Records of the Australian Museum Supplement* 1993;**19**:1–77. https://doi.org/10.3853/j.0812-7387.19.1993.52
Koch NM, Parry LA. Death is on our side: paleontological data drastically modify phylogenetic hypotheses. *Systematic Biology* 2020;**69**:1052–67. https://doi.org/10.1093/sysbio/syaa023
Krefft G. Description of *Aspidiotes melanocephalus*, a new snake from Port Denison. *Proceedings of the Zoological Society of London* 1864;**1864**:20–2.
Krishtalka L, West RM, Black CC, *et al*. Eocene (Wasatchian through Duchesnean) biochronology of North America. In: Woodburne MO (ed.), *Cenozoic Mammals of North America: Geochronology and Biostratigraphy*. Berkeley: University of California Press, 1987, 77–117.
Krumbiegel G, Rule L, Haubold H. *Das Eozäne Geiseltal. Ein mitteleuropäisches Braunkohlenvorkommen und seine Planzen- und Tierwelt*. Wittenberg Lutherstadt: A. Ziemsen Verlag, 1983.
Krutzsch W. Die sporenstratigraphische Gliederung des Tertiarim nordlichen Mitteleuropa (Palaozan-Mitteloligozan), methodische Grundlagen und gegenwartiger Stand der Untersuchungen. *Abhandlungen des Zentralen Geologischen Instituts* 1966;**8**:112–49.
Krutzsch W. Die stratigraphisch verwertbaren Sporen- und Pollenformen des mitteleuropaischen Alttertiars. *Jahrbuch fur Geologie* 1970;**3**:309–79.
Krutzsch W. Die stratigraphische Stellung des Geiseltalprofils im Eozän und die sporenstratigraphische Untergliederung des mittleren Eozäns. *Abhandlungen des Zentral Geologischen Instituts, Paläontologische Abhandlungen* 1976;**26**:47–92.
Krutzsch W, Blumenstengel H, Kiesel Y *et al*. Palaobotanische Klimagliederung des Alttertiars (Mitteleozan bis Oberoligozan) in Mitteldeutschland und das Problem der Verknupfung mariner und kontinentaler Gliederungen (klassische Biostratigraphien-palaobotanisch-okologische Klimastratigraphie-Evolutionsstratigraphie der Vertebraten). *Neues Jahrbuch fur Geologie und Palaontologie, Abhandlungen* 1992;**186**:137–253.
Kuhn O. Die Schlangen (Boidae) aus dem Mitteleozän des Geiseltales. *Nova Acta Leopoldina, Neue Folge* 1939;**7**:119–33.
Kuhn O. Die Placosauriden und Anguiden aus dem Mittleren Eozän des Geiseltales. *Nova Acta Academia Leopoldina, Carolinska* 1940;**53**:461–86.
Kuhn O. Weitere Lacertilier, insbesondere Iguanidae aus dem Eozän des Geiseltales. *Paläontologische Zeitschrift* 1944;**23**:360–7. https://doi.org/10.1007/bf03160444
Lanfear R, Frandsen PB, Wright AM *et al*. PartitionFinder 2: new methods for selecting partitioned models of evolution for molecular and morphological phylogenetic analyses. *Molecular Biology and Evolution* 2017;**34**:772–3. https://doi.org/10.1093/molbev/msw260
Lenz OK, Wilde V, Mertz DF *et al*. New palynology-based astronomical and revised $^{40}Ar/^{39}Ar$ ages for the Eocene maar lake of Messel (Germany). *International Journal of Earth Sciences* 2015;**104**:873–89. https://doi.org/10.1007/s00531-014-1126-2
Lewis PO. A likelihood approach to estimating phylogeny from discrete morphological character data. *Systematic Biology* 2001;**50**:913–25. https://doi.org/10.1080/106351501753462876
Linnaeus C. *Systema Naturae per Regna tria Naturae, Secundum Classes, Ordines, Genera, Species, cum Characteribus, Differentiis, Synonymis, Locis*. Stockholm: Laurentii Salvii, 1758.
Maddison WP, Maddison DR. Mesquite: a modular system for evolutionary analysis. Version 3.31. 2019. Available at: https://mesquiteproject.org
Marsh OC. Description of some new fossil serpents from the Tertiary deposits of Wyoming. *American Journal of Sciences, Series 3* 1871;**s3-1**:322–9. https://doi.org/10.2475/ajs.s3-1.5.322
Marsh OC. Notice of new reptiles from the Laramie Formation. *American Journal of Science* 1892;**s3-43**:449–53. https://doi.org/10.2475/ajs.s3-43.257.449
Mayr G. An updated review of the middle Eocene avifauna from the Geiseltal (Germany), with comments on the unusual taphonomy of some bird remains. *Geobios* 2020;**62**:45–59. https://doi.org/10.1016/j.geobios.2020.06.011
McCartney JA, Seiffert ER. A Late Eocene snake fauna from the Fayum Depression, Egypt. *Journal of Vertebrate Paleontology* 2016;**36**:e1029580. https://doi.org/10.1080/02724634.2015.1029580
McKenna MC. Cenozoic paleogeography of North Atlantic land bridges. In: Bott MHP, Saxov S, Talwani M, Thiede J (eds), *Structure and Development of the Greenland–Scotland Ridge: New Methods and Concepts*. New York: Plenum Press, 1983, 351–399.
Młynarski M. Bemerkungen über die Schildkröten (Testudines) des Geiseltales. *Wissenschaftliche Beiträge der Martin-Luther-Universität Halle-Wittenberg* 1977;**5**:99–105.
Müller F. Erster Nachtrag zum Katalog der herpetologischen Sammlung des Basler Museums. *Verhandlungen der Naturforschenden Gesellschaft in Basel* 1880;**7**:120–65.
O'Shea M. *Boas and Pythons of the World*. Princeton: Princeton University Press, 2007.
Onary S, Hsiou AS, Lee MSY *et al*. Redescription, taxonomy and phylogenetic relationships of *Boavus* Marsh, 1871 (Serpentes: Booidea) from the early–middle Eocene of the USA. *Journal of Systematic Palaeontology* 2022;**19**:1601–22. https://doi.org/10.1080/14772019.2022.2068386
Oppel M. *Die Ordnungen, Familien und Gattungen der Reptilien als Prodrom Einer Naturgeschichte Derselben*. Munich: Lindauer, 1811a.
Oppel M. Suite du 1er memoire sur la classification des reptiles Ord II Squammata mihi Sect II Ophidii Ord III Ophidii, Brongniart. *Annales du Museum d'histoire Naturelle, Paris* 1811b;**16**:376–93.
Owen R. Part III. Ophidia (*Palaeophis* & c.). In: Owen R (ed.), *Monograph on the Fossil Reptilia of the London Clay and of the Bracklesham and other Tertiary beds*. London: Palaeontographical Society of London, 1850, 51–63.
Palci A, Caldwell MW. Primary homologies of the circumorbital bones of snakes. *Journal of Morphology* 2013;**274**:973–86. https://doi.org/10.1002/jmor.20153
Pérez García A, Lapparent de Broin FD, Murelaga X. The *Erymnochelys* group of turtles (Pleurodira, Podocnemididae) in the Eocene of Europe: new taxa and paleobiogeographical implications. *Palaeontologica Electronica* 2017;**20**:1–28.
Pyron RA. Post-molecular systematics and the future of phylogenetics. *Trends in Ecology & Evolution* 2015;**30**:384–9. https://doi.org/10.1016/j.tree.2015.04.016
Pyron RA, Burbrink FT, Wiens JJ. A phylogeny and revised classification of Squamata, including 4161 species of lizards and snakes. *BMC Evolutionary Biology* 2013;**13**:93. https://doi.org/10.1186/1471-2148-13-93
Pyron RA, Reynolds RG, Burbrink FT. A taxonomic revision of boas (Serpentes: Boidae). *Zootaxa* 2014;**3846**:249–60. https://doi.org/10.11646/zootaxa.3846.2.5
Rabi M, Sebők N. A revised Eurogondwana model: Late Cretaceous notosuchian crocodyliforms and other vertebrate taxa suggest the retention of episodic faunal links between Europe and Gondwana during most of the Cretaceous. *Gondwana Research* 2015;**28**:1197–211. https://doi.org/10.1016/j.gr.2014.09.015
Rage J-C. Fossil snakes from the Paleocene of São José de Itaboraí, Brazil. Part II. Boidae. *Palaeovertebrata* 2001;**30**:111–50.
Rage J-C. Fossil snakes from the Paleocene of São José de Itaboraí, Brazil. Part III. Ungaliophiinae, Booids incertae sedis, and Caenophidia. Summary, update, and discussion of the snake fauna from the locality. *Palaeovertebrata* 2008;**36**:37–73.
Rage J-C, Adaci M, Bensalah M *et al*. Latest Early-Early Middle Eocene deposits of Algeria (Glib Zegdou, HGL50), yield the richest and

most diverse fauna of amphibians and squamate reptiles from the Palaeogene of Africa. *Palaeovertebrata* 2021;**44**:e1–32. https://doi.org/10.18563/pv.44.1.e1

Rambaut A, Drummond AL, Xie D *et al.* Posterior summarization in Bayesian phylogenetics using tracer 17. *Systematic Biology* 2018;**67**:901–4. https://doi.org/10.1093/sysbio/syy032

Reynolds RG, Niemiller ML, Revell LJ. Toward a tree-of-life for the boas and pythons: Multilocus species-level phylogeny with unprecedented taxon sampling. *Molecular Phylogenetics and Evolution* 2014;**71**:201–13. https://doi.org/10.1016/j.ympev.2013.11.011

Rieppel O. The evolution of the basicranium in the Henophidia (Reptilia: Serpentes). *Zoological Journal of the Linnean Society* 1979;**66**:411–31. https://doi.org/10.1111/j.1096-3642.1979.tb01915.x

Ring SJ, Bocherens H, Wings O *et al.* Divergent mammalian body size in a stable Eocene greenhouse climate. *Scientific Reports* 2020;**10**:1–10. https://doi.org/10.1038/s41598-020-60379-7

Roček Z, Wuttke M, Gardner JD *et al.* The Euro-American genus *Eopelobates*, and a re-definition of the family Pelobatidae (Amphibia, Anura). *Palaeobiodiversity and Palaeoenvironments* 2014;**94**:529–67. https://doi.org/10.1007/s12549-014-0169-5

Rochebrune AT. Revision des ophidiens fossiles du Museum d'Histoire Naturelle. *Nouvelles Archives du Museum d'Histoire Naturelle, 2eme Serie* 1880;**3**:271–96.

Ronquist F, Teslenko M, Van Der Mark P *et al.* MrBayes 32: efficient Bayesian phylogenetic inference and model choice across a large model space. *Systematic Biology* 2012;**61**:539–42. https://doi.org/10.1093/sysbio/sys029

Rossmann T. Osteologische Beschreibung von *Geiseltaliellus longicaudus* Kuhn, 1944 (Squamata: Iguanoidea) aus dem Mittleren Eozän der Fossillagerstätten Geiseltal und Grube Messel (Deutschland), mit einer Revision der Gattung. *Geiseltaliellus, Palaeontographica A* 2000;**258**:117–58.

Russell P. *A Continuation of an Account of Indian Serpents: Containing Descriptions and Figures from Specimens and Drawings, Transmitted from Various Parts of India to the Hon. Court of Directors of the East Indian Company*. Volume **2**. London: W. Bulmer and Co. Shakespeare-Press, 1801.

Salzmann W. *Das Braunkohlenvorkommen im Geiseltal mit Besonderer Berücksichtigung der Genesis*. Berlin: Königlich Preußische Geologische Landesanstalt, 1914.

Scanferla A, Smith KT. Exquisitely preserved fossil snakes of Messel: insight into the evolution, biogeography, habitat preferences and sensory ecology of early boas. *Diversity* 2020a;**12**:100. https://doi.org/10.3390/d12030100

Scanferla A, Smith KT. Additional anatomical information on the Eocene minute boas *Messelophis variatus* and *Rieppelophis ermannorum* (Messel Formation, Germany). *Vertebrate Zoology* 2020b;**70**:615–20. https://doi.org/10.26049/VZ70-4-2020-06

Scanferla A, Smith KT, Schaal SF. Revision of the cranial anatomy and phylogenetic relationships of the Eocene minute boas *Messelophis variatus* and *Messelophis ermannorum* (Serpentes, Booidea). *Zoological Journal of the Linnean Society* 2016;**176**:182–206. https://doi.org/10.1111/zoj.12300

Schaal S. *Palaeopython fischeri* n. sp. (Serpentes: Boidae), eine Riesenschlange aus dem Eozän (MP 11) von Messel. *Courier Forschungsinstitut Senckenberg* 2004;**252**:35–45.

Schaal S, Baszio S. *Messelophis ermannorum* n. sp., eine neue Zwergboa (Serpentes: Boidae: Tropidopheinae) aus dem Mittel-Eozän von Messel. *Courier Forschungsinstitut Senckenberg* 2004;**252**:67–77.

Schlegel H. *Essai sur la Physionomie des Serpens*. Amsterdam: Schonekat MH, Librairie-Éditeur, 1837.

Schlegel H. Description d'une nouvelle espèce du genre eryx, *Eryx reinhardtii. Bijdragen tot de Dierkunde* 1851;**1**:1–3.

Schlegel H. *De direntium van het Koninklijk Zoologisch Genootschap Natura Artis Magistra te Amsterdam, Reptilia*. Amsterdam: Van Es, 1872.

Schneider JG. *Historiae Amphibiorum Naturalis et Literariae, Fasciculus Secundus Continens Crocodilos, Scincos, Chamaesauras, Boas, Pseudoboas, Elapes, Angues, Amphisbaenas et Caecilias*. Jena: Wesselhoeft, 1801.

Scotese CR. *Atlas of Paleogene Paleogeographic Maps (Mollweide Projection), Maps 8-15, Volume 1, The Cenozoic, Paleomap Atlas for ArcGIS*. Evanston, IL: Paleomap Project, 2014.

Segall M, Palci A, Skipwith P, *et al.* Chapter 1: Evolution of the form and function of the head of snakes. In: Penning D (ed.), *Snakes: Morphology, Function, and Ecology*. New York: Nova Science Publishers, pp. 1–70; 2023.

Smith KT. Eocene lizards of the clade *Geiseltaliellus* from Messel and Geiseltal, Germany, and the early radiation of Iguanidae (Squamata: Iguania). *Bulletin of the Peabody Museum of Natural History* 2009;**50**:219–306. https://doi.org/10.3374/014.050.0201

Smith KT. New constraints on the evolution of the snake clades Ungaliophiinae, Loxocemidae and Colubridae (Serpentes), with comments on the fossil history of erycine boids in North America. *Zoologischer Anzeiger - A Journal of Comparative Zoology* 2013;**252**:157–82. https://doi.org/10.1016/j.jcz.2012.05.006

Smith KT, Georgalis GL. The diversity and distribution of Palaeogene snakes: a review, with comments on vertebral sufficiency. In: Gower D, Zaher H (eds), *The Origin and Early Evolution of Snakes*. Cambridge: Cambridge University Press, 2022, 55–84. https://doi.org/10.1017/9781108938891.006

Smith KT, Scanferla A. Fossil snake preserving three trophic levels and evidence for an ontogenetic dietary shift. *Palaeobiodiversity and Palaeoenvironments* 2016;**96**:589–99. https://doi.org/10.1007/s12549-016-0244-1

Smith KT, Scanferla A. A nearly complete skeleton of the oldest definitive erycine boid (Messel, Germany). *Geodiversitas* 2021;**43**:1–24. https://doi.org/10.5252/geodiversitas2021v43a1

Smith KT, Scanferla A. More than one large constrictor lurked around paleolake Messel. *Palaeontographica, Abteilung A: Palaeozoology – Stratigraphy* 2022;**323**:75–103. https://doi.org/10.1127/pala/2021/0119

Smith KT, Schaal SFK, Habersetzer J. *Messel: An Ancient Greenhouse Ecosystem*. Stuttgart: Schweizerbart, 2018.

Solé F, Smith T, Tabuce R *et al.* New dental elements of the oldest proviverrine mammal from the Early Eocene of southern France support possible African origin of the subfamily. *Acta Palaeontologica Polonica* 2015;**60**:527–38. https://doi.org/10.4202/app.00146.2014

Steinheimer FD, Hastings AK. Halle: the Geiseltal collection of Martin Luther University, Halle-Wittenberg. In: Beck LA, Joger U (eds), *Paleontological Collections of Germany, Austria and Switzerland*. Cham: Springer, 2018, 271–280.

Swofford DL. PAUP*. Phylogenetic Analysis Using Parsimony (* and Other Methods). Version 4. Sinauer Associates, Sunderland, *Massachusetts* 2003. https://paup.phylosolutions.com/

Szyndlar Z, Georgalis GL. An illustrated atlas of the vertebral morphology of extant non-caenophidian snakes, with special emphasis on the cloacal and caudal portions of the column. *Vertebrate Zoology* 2023;**73**:717–886. https://doi.org/10.3897/vz.73.e101372

Tonini JFR, Beard KH, Ferreira RB *et al.* Fully-sampled phylogenies of squamates reveal evolutionary patterns in threat status. *Biological Conservation* 2016;**204**:23–31. https://doi.org/10.1016/j.biocon.2016.03.039

Villa A, Wings O, Rabi M. A new gecko (Squamata, Gekkota) from the Eocene of Geiseltal (Germany) implies long-term persistence of European Sphaerodactylidae. *Papers in Palaeontology* 2022;**8**:e1434. https://doi.org/10.1002/spp2.1434

Wagler JG. Auszüge aus seinem Systema Amphibiorum. *Isis von Oken* 1828;**21**:740–4.

Walter J, Darlim G, Massonne T *et al.* On the origin of Caimaninae: insights from new fossils of *Tsoabichi greenriverensis* and a review of the evidence. *Historical Biology* 2021;**34**:580–95. https://doi.org/10.1080/08912963.2021.1938563

Wells RW, Wellington CR. A synopsis of the class Reptilia in Australia. *Australian Journal of Herpetology* 1984;**1**:73–129.

Zaher H, Smith KT. Pythons in the Eocene of Europe reveal a much older divergence of the group in sympatry with boas. *Biology Letters* 2020;**16**:20200735. https://doi.org/10.1098/rsbl.2020.0735

Zaher H, Mohabey DM, Grazziotin FG *et al*. The skull of *Sanajeh indicus*, a Cretaceous snake with an upper temporal bar, and the origin of ophidian wide-gaped feeding. *Zoological Journal of the Linnean Society* 2023;**197**:656–97. https://doi.org/10.1093/zoolinnean/zlac001

Zheng Y, Wiens JJ. Combining phylogenomic and supermatrix approaches, and a time-calibrated phylogeny for squamate reptiles (lizards and snakes) based on 52 genes and 4162 species. *Molecular Phylogenetics and Evolution* 2016;**94**:537–47. https://doi.org/10.1016/j.ympev.2015.10.009